Multimedia Tools and Applications (2019) 78:35733–35788
https://doi.org/10.1007/s11042-019-08195-8

An efficient optimal multilevel image thresholding with electromagnetism-like mechanism

Ashish Kumar Bhandari[1] · Neha Singh[1] · Swapnil Shubham[1]

Received: 16 February 2019 / Revised: 24 July 2019 / Accepted: 6 September 2019
Published online: 5 October 2019

Abstract
Segmentation process is considered a major part of various image-processing applications due to its extreme inspiration on the subsequent image analysis. Thresholding is one of the simplest techniques for segmentation. In this paper, Renyi's entropy is combined with electromagnetism-like mechanism optimization (EMO) to perform multilevel thresholding based color image segmentation. For statistical independent subsystems, Renyi's entropy shows an extensive property and is applied to find best threshold value for image segmentation. The entropic parameter α can handle the additive information that is existent in the image. The feasibility of the EMO-Renyi's based approach has been tested on various satellite and standard color images with bat algorithm (BAT), backtracking search algorithm (BSA), firefly algorithm (FA), particle swarm optimization (PSO), and wind driven optimization (WDO) for solving the multilevel color image thresholding problem. The analysis based on statistics of different optimization algorithms indicates the proposed EMO-Renyi's algorithm to be more robust and precise for multilevel color image segmentation problem. These claims have been confirmed by comparing fidelity parameters such as mean error (ME), mean squared error (MSE), peak signal-to-noise ratio (PSNR), feature similarity index (FSIM), structure similarity index (SSIM) and entropy. Experiments on standard daily-life color images are conducted to prove the effectiveness of the proposed scheme. The results show that the proposed method can produce more promising segmentation results from the aspect of objective and subjective observations.

Keywords Image segmentation · Electromagnetism-like mechanism · Renyi's entropy · Tsallis entropy · Kapur's entropy

1 Introduction

The classification of pixels into two or more regimes defines segmentation. The region of interest in the image can be efficiently extracted and analyzed using image segmentation. To

✉ Ashish Kumar Bhandari
bhandari.iiitj@gmail.com

Extended author information available on the last page of the article

carry out the segmentation of an image, the presence of mutual information in the sub-regions is necessary. The mutual information could be any of the attributes such as texture, color, and shape [1]. The successful implementation of image segmentation in several areas such as agriculture [15], image denoising [27], industrial production [20], medical image processing [21, 48], and pattern recognition [58] has made. Segmentation methods can be categorized into region-based segmentation [16, 32], threshold-based segmentation [3, 26], edge-based segmentation [4, 5, 47], and clustering techniques [2] to name a few. Image segmentation based on thresholding [53] has its application on a histogram of the image [14]. This results in the consumption of less storage space, proficient processing speed and easy handling which makes the thresholding based segmentation approach as the most frequently used method for segmentation.

Generally, the thresholding techniques are classified into two parts named as bi-level and multilevel thresholding. The process of dividing the entire image into two non-overlapping regimes using a single threshold is termed as bi-level thresholding. According to the predefined threshold value *th*, the pixels representing the gray levels below the intensity value *th* belongs to one class viz. background while other pixels belong to another class. On the other hand, multilevel thresholding is done using more than one threshold which implies that there are more than 2 classes. Although bi-level thresholding method is one of the simplest and easiest technique however, for daily life color images and remote sensing data set it doesn't give appropriate results. As a consequence, multi-level thresholding has a strong obligation for color image segmentation. Thresholding methods can be categorized into non-parametric methods and parametric methods. The parameter estimation of a probability density function (PDF) is a necessity in parametric approaches. Such an approach is resource-intensive. On the contrary, a non-parametric technique employs statistical properties for threshold selection [51] based on the image histogram such as between-class variance-based methods [40], moment-based technique [56] and entropy-based approach [33].

These statistical parameters must be optimized to determine the optimum threshold values. The non-parameterized approach opens a striking option due to its exactness and robustness [6]. Counter production of between-class variance adds to the consumption in the computational cost of an algorithm specifically in multi-level threshold selection. Amongst all the remarkable thresholding methods, thresholding based on entropy is an absorbing subject. Kapur et al. [33] proposed a method that uses the model of entropy maximization to determine the homogeneousness between classes. The information in the image can be treated as either additive or the non-additive. A maximum entropy method has been proposed on the basis of non-extensive Tsallis entropy [23] whose entropic parameter q enables the Tsallis entropy to handle the non-additive information.

In 1997, Sahoo [52] has proposed a method for thresholding based on Renyi's entropy. Renyi's entropy can handle the additive property using the tuneable entropic parameter α [31, 50]. The value of α and q can be varied to maximize the Renyi's and Tsallis entropy respectively. A simple implementation of Renyi's entropy is the motivation behind its exploitation. The easy extension of Renyi's entropy to multilevel thresholding problems sums up the advantage of less computation cost. The results show that the accuracy of Renyi's entropy surpasses that of Tsallis entropy and Kapur's entropy. Therefore, in this paper, Renyi's entropy is selected for the entropy computation due to its superlative accuracy and enhanced performance for the purpose of color image segmentation. However, the classical multilevel color image thresholding methods based on entropy results in the huge consumption of time when the thresholding level increases. A substitute for traditional methods, the multi-level

thresholding problems have also been managed through swarm-based evolutionary optimization methods. Over the last few years, the success of utilization of meta-heuristic algorithms is one to note. The swarm and evolutionary methodologies have been successful in solving the problem of multilevel image segmentation to achieve the optimum multilevel threshold.

Furthermore, numerous optimization based thresholding techniques have been established which use the features of swarm and evolutionary techniques viz. artificial bee colony (ABC) inspired from the searching behaviour of swarm of honey bees [7, 9, 30], genetic algorithm (GA) which is motivated from the notion of survival of the fittest given by Darwin [9], PSO based on public behaviour of fish schooling or bird flocking [11]. In addition to this, FA is based on flashing phenomenon of fireflies of tropical areas during summer season [28, 29], WDO other optimization methodology which is grounded on the atmospheric behaviour of earth [8, 11], EMO has been inspired from the attraction-repulsion mechanism of the electromagnetism theory [38, 39].

The concept on which the BAT algorithm relates to the echolocation of the bats [36, 41]. In 2017, a new color image multilevel thresholding has been proposed by exploiting the backtracking search algorithm (BSA) for satellite images [22, 25, 44]. In favor of color image multilevel thresholding, another new approach has been given [45] through the modification of fuzzy entropy and further the proposed modified entropic parameters are optimized by Levy flight firefly algorithm to get more accurate results for satellite image segmentation. On the other hand, a new grey-level co-occurrence matrix [46] has been introduced first time as an objective function to get accurate multilevel thresholding for multiband remote sensing images as well as daily life color images. Ant colony optimization (ACO) [25], cuckoo search (CS) [8, 43], bacterial foraging optimization (BFO) [49], differential evolution (DE) [13], and honey bee mating optimization [57] have been reported explicitly to many multilevel color image segmentation problems for evaluation of optimal thresholds.

The swarm-based algorithms [11] and evolutionary computing approaches [12, 42] outstand due to their ability to search superlative solution from any of the objective functions. In 2015, Bhandari et al. [10] has proposed a novel method based on CS methodology for the problem of color image segmentation which is supported by Tsallis entropy. Renyi's entropy has been used by Soham et al. [53] while proposing a technique to segment the hyper-spectral images with the aid of differential evolution. Again in 2016, a comparative performance analysis [41] using two new optimization algorithms, social spiders optimization (SSO) and flower pollination algorithm (FPA) has been done by taking Kapur's and Otsu's as the fitness functions. The two functions, Kapur's and Otsu's have also been used to perform multilevel color image thresholding using EMO [38] technique, which shows that EMO algorithm gives more satisfactory results with Otsu as objective function when compared with that of Kapur's.

Again in 2015, Oliva et al. [39] has used the electromagnetism-like mechanism optimization method to speed up the segmentation process and this time Tsallis entropy has been used as a fitness function. Multilevel thresholding for iris images has been done based on the artificial bee colony [19]. Recently, a modified PSO [35] based multilevel thresholding is applied for the segmentation of medical image segmentation. PSO has been used again in Glioma detection based on multi-fractal features in the medical field to segmented brain MRI images [34]. Lifan et al. [29] presented a work of multilevel color image thresholding by modifying the firefly algorithm and used Kapur's, minimum cross-entropy and Otsu's as objective (or fitness) function.

Shilpa et al. have proposed an effectual CS algorithm based thresholding for segmentation of remote sensing images using various objective functions [54] and also proposed multilevel

thresholding that is based on chaotic Darwinian PSO for segmentation of satellite images [55]. In 2016, Pare et al. proposed a technique for multilevel color image segmentation using CS and energy curve concept [43]. Unlike segmentation for satellite images, segmentation of dental X-ray images has been proposed based on cooperative semi-supervised fuzzy clustering [48]. Satellite images have always been a study of interest in fields such as astronomical studies, geoscience studies, a survey of climate, forest monitoring, geographical system, agriculture and marine environment [9, 11]. Therefore, for providing the solutions to such king of problems, in this paper, BAT algorithm, BSA, FA, PSO, WDO and EMO based satellite image segmentation using Kapur's, Tsallis and Renyi entropy is inspected. The schemes are used to maximize the entropy as a fitness function.

This paper is focused on EMO algorithm is used for the proposed approach due to its novelty and an ability of the solving real constraints. The electromagnetism-like mechanism optimization method is used to speed up the segmentation process. This optimization technique generates good results for test functions such as unimodal, multi-modal, and composite and balances global and local search during optimization. In addition to this Renyi's entropy has selected for entropy computation because of the easiest implementation. The Renyi's entropy has additive features. The entropic parameter α is used to maximize the entropy. The easy extension of Renyi's entropy along with producing accurate results as compared to Kapur's and Tsallis entropy so it is nominated for the entropy computation. Furthermore, by incorporating Renyi's entropy with EMO technique, it reduces the complexity cost and produces accurate segmented enhanced result. Hence, several researchers are focused on EMO algorithm in their respective research areas for good results with high convergence rate.

The remainder of the paper is organized as follows: Section 2 describes the concepts related to the proposed scheme and the problem statement. Section 3 presents the EMO and Renyi entropy-based proposed framework. Section 4 highlights the comparison of the entropy using each optimization algorithm. Finally, conclusion and future work are drawn in Section 5.

2 Problem statement for optimal multilevel thresholding

Global thresholding can be defined using Eq. (1). If $g(x, y)$ is the original image and $f(x, y)$ represents the thresholded version of the original image then at some global threshold Th can be expressed as:

$$f(x,y) = \left\{ \begin{array}{l} 0; \mathrm{g}(x,y) \leq Th \\ 1; \mathrm{g}(x,y) > Th \end{array} \right\}, \tag{1}$$

where, (x, y) represents the pixel location. The variation of Th over the entire image gives variable thresholding. When Th is a function of the pixel location (x, y) adaptive thresholding can be done and if Th has a dependency on the neighboring pixels, regional thresholding or local thresholding can be evaluated.

2.1 Thresholding

The pixels of a gray-scale or colored image are classified into regions or sets on account of their intensity level (L). For the selection of fitting neighborhoods in a test image, the optimum

threshold value Th should be obtained in a routine, which obeys the simple law of the following equations:

$$\begin{aligned} C_0 &\leftarrow i \;\; if \;\; 0 \le i \le Th, \\ C_1 &\leftarrow i \;\; if \;\; Th \le i \le L-1 \end{aligned} \tag{2}$$

and

$$\begin{aligned} C_0 &\leftarrow i \;\; if \;\; 0 \le i < Th_1 \\ C_1 &\leftarrow i \;\; if \;\; Th_1 \le i < Th_2, \\ C_2 &\leftarrow i \;\; if \;\; Th_2 \le i < Th_3, \\ C_n &\leftarrow i \;\; if \;\; Th_n \le i \le L-1, \end{aligned} \tag{3}$$

where, C_0 to C_n defines the classes of the image after thresholding operation is done, i represent the intensity value of the image with the maximum intensity value L and $\{Th_1, Th_2, Th_3, \ldots, Th_n\}$ represents multiple thresholds.

Segmentation of pixels in their respective classes is done using Eqs. (2) and (3) for bi-level thresholding and multilevel thresholding respectively. The core idea is to choose threshold values that properly classify the different regions in the image using either of bi-level or multilevel thresholding algorithms. When the problem's formulation is considered, it has been observed that the two-level thresholding is a simple technique for the purpose of obtaining a threshold for segmentation. However, estimating thresholds for multilevel thresholding requires higher computational works.

2.2 Kapur's entropy-based segmentation

The Kapur's method aims at maximizing the entropy such that each different region has greater centralized distribution. Kapur's entropy [33] based thresholding methodology is cited as an effective method. Furthermore, Kapur's entropy [8] has been extended for multilevel thresholding problem [37] as represented by Eq. (4):

$$\begin{aligned} E_{k0} &= -\sum_{i=0}^{Th_1-1} \frac{h_i}{w_0} \ln \frac{h_i}{w_0}, w_0 = \sum_{i=0}^{Th_1-1} h_i, \\ E_{k1} &= -\sum_{i=Th_1}^{Th_2-1} \frac{h_i}{w_1} \ln \frac{h_i}{w_1}, w_1 = \sum_{i=Th_1}^{Th_2-1} h_i, \\ E_{km} &= -\sum_{i=Th_m}^{Th_{m+1}-1} \frac{h_i}{w_m} \ln \frac{h_i}{w_m}, w_m = \sum_{i=Th_m}^{Th_{m+1}-1} h_i, \\ E_{kn} &= -\sum_{i=Th_n}^{L-1} \frac{h_i}{w_n} \ln \frac{h_i}{w_n}, w_n = \sum_{i=Th_n}^{L-1} h_i, \end{aligned} \tag{4}$$

where, E_{ki} represents the Kapur's entropy of i_{th} class, w_i represents the probability of i_{th} class and n represents the maximum number of classes.

The optimal multilevel segmentation problem is solved by considering it as an n-dimensional problem of optimization. Now, to solve the multilevel thresholding problem, n-dimensional optimal thresholds are obtained by Eq. (5), which is used for the maximization of the objective function as:

$$(t)^* = \arg\max\left(\sum_{i=0}^{n} E_{ki}\right). \tag{5}$$

2.3 Concept of Tsallis entropy for segmentation

Constantino Tsallis have proposed the Tsallis entropy. The concept of Tsallis entropy is based on the Shannon's entropy. Discrete probabilities make up the fundamental principle for Tsallis entropy where the sum of total of all discrete probabilities is 1. Tsallis entropy is capable of handling non-additive or non-extensive information [9, 10]. The entropy for a class is calculated using Eq. (6):

$$E_T = \frac{1}{1-q}\left[\sum_{i=0}^{Th}\left(\frac{h_i}{w_0}\right)^q - 1\right]. \tag{6}$$

The maximized Tsallis entropy can be achieved by using Eq. (7) which can be presented as:

$$E_T = E_{T0} + E_{T1} + E_{T2} + \ldots + E_{Tn} + (1-q)\, E_{T0}E_{T1}E_{T2}\ldots E_{Tn}, \tag{7}$$

where,

$$\begin{aligned}
E_{T0} &= \frac{1}{1-q}\left[\sum_{i=0}^{Th_1-1}\left(\frac{h_i}{w_0}\right)^q - 1\right], w_0 = \sum_{i=0}^{Th_1-1} h_i,\\
E_{T1} &= \frac{1}{1-q}\left[\sum_{i=Th_1}^{Th_2-1}\left(\frac{h_i}{w_1}\right)^q - 1\right], w_1 = \sum_{i=Th_1}^{Th_2-1} h_i,\\
E_{T2} &= \frac{1}{1-q}\left[\sum_{i=Th_2}^{Th_3-1}\left(\frac{h_i}{w_2}\right)^q - 1\right], w_2 = \sum_{i=Th_2}^{Th_3-1} h_i,\\
E_{Tn} &= \frac{1}{1-q}\left[\sum_{i=Th_n}^{L-1}\left(\frac{h_i}{w_n}\right)^q - 1\right], w_n = \sum_{i=Th_n}^{L-1} h_i,
\end{aligned} \tag{8}$$

where, E_{Ti} represents the Tsallis entropy of i_{th} class and n represents the maximum number of classes. The values of Eq. (8) give the Tsallis entropy of each region (or class) and these values are used in Eq. (7) to get the maximum entropic value. This degree of non-additivity is represented by the variable q which behaves as an entropic parameter. When the value of q is taken to be 1, the Tsallis entropy reduces to the Shannon entropy which implies that the Tsallis entropy is derived from of Shannon entropy. In this paper, the value of q is considered as 0.8 for each optimization algorithm to maximize the Tsallis entropy. In this context, the BAT [36, 41], BSA [22, 25, 44], FA [28, 29], PSO [11], and WDO [8] algorithms are used as optimization techniques to determine the optimum thresholds for segmentation which are obtained by maximizing each entropy as fitness functions. Through which evaluation of precision of the segmented image has been done.

3 Proposed algorithm

In this paper, the segmentation process is carried out with an optimization methodology that is presented as:

$$\text{maximize } f_{Kapur}(Th) \text{ or } f_{Tsallis}(Th),\ Th = [Th_1, Th_2, \ldots, Th_n], \tag{9}$$

where, Th_1, Th_2,…,Th_n define the thresholds which are used for segmentation purpose. In the presented method, the segmentation of an image is processed with an optimization technique that is formulated as Eq. (10):

$$\text{maximize } f_{Renyi}(TH), Th = [Th_1, Th_2, \ldots, Th_n], \text{where, } TH \in X = \left\{R^k \mid 0 \leq Th_i \leq 255\right\}. \quad (10)$$

Where $i = [1, 2, \ldots, n]$ and X denotes the constrained region which is valid for the interval 0 to 255.

Therefore, the Renyi's entropy-based EMO algorithm is utilized in order to search the gray level values (TH), which can resolve the formulated problem of multilevel thresholding. Optimization refers to the process of obtaining the best possible outcome for a method, which should be better than the previous result. A block diagram for an overall process of optimal color image multilevel thresholding using optimization techniques is demonstrated in Fig. 1.

3.1 Renyi based thresholding

Alfred Renyi proposed a definition for the measure of information that preserves the expansively for independent events which later termed as Renyi's entropy. This entropy quantifies the randomness, uncertainty or diversity of a system. Renyi entropy is used as a diversity index in statistics and ecology and also essential in quantum information where it is used to measure entanglement [31, 52]. The entropic parameter α defines the amount of extensive information that is present in the image. In a system, the value of α determines which events contribute to the calculation of Renyi's entropy. For example, if the value of α tends to 0, almost all the events are weighted equally by Renyi's entropy and if a value of α tends to infinity, Renyi entropy is evaluated using the events that have the highest probability.

Similarly, in the case of image processing, the events represent the classes of the image whose probabilities are used to determine Renyi's entropy. When the value of α is closer to zero, regardless of the probability of each class, Renyi entropy weighs all possible events more equally and when α is one, Renyi entropy reduces to Shannon entropy. This entropy yields maximum result when the value of α is taken to be 0.8. Renyi entropy can be presented using Eq. (11)

$$E_R = \frac{1}{1-\alpha} \ln \sum_{i=0}^{Th} \left(\frac{h_i}{w_0}\right)^{\alpha}, \quad (11)$$

where, E_R defines the entropy of a class.

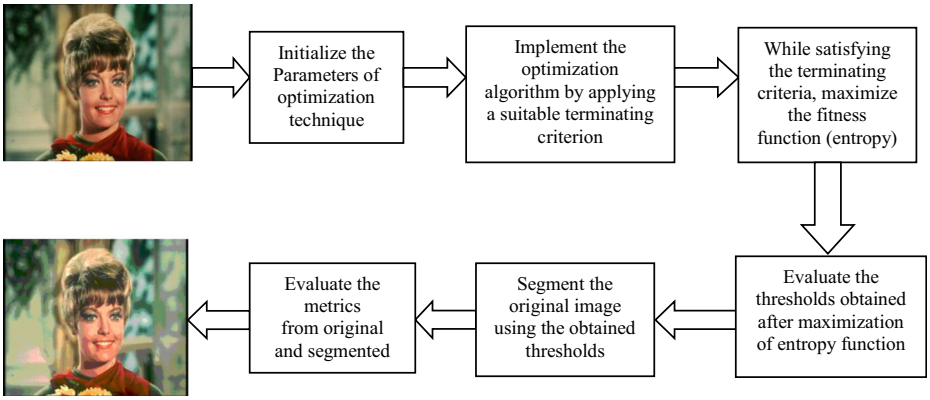

Fig. 1 Block diagram of the multilevel thresholding using optimization techniques

Renyi entropy is a monotonically decaying function of given probability distribution in accordance with α [31]. As already detailed, Renyi entropy satisfies the additive property which can be expressed as then the total Renyi entropy of the system is given by

$$E_R(C_0 + C_1) = E_R(C_0) + E_R(C_1), \tag{12}$$

where, $E_R(C_0)$ represents Renyi entropy of class C_0. This additive property can be extended to n independent classes $C0$, $C1$, $C2$, ...,C_n by

$$E_R(C_0 + C_1 + C_2 + \ldots + C_n) = E_R(C_0) + E_R(C_1) + E_R(C_2) + \ldots + E_R(C_n), \tag{13}$$

where

$$\begin{aligned}
E_{R0} &= \frac{1}{1-\alpha}\ln \sum_{i=0}^{Th_1-1}\left(\frac{h_i}{w_0}\right)^{\alpha}, w_0 = \sum_{i=0}^{Th_1-1} h_i,\\
E_{R1} &= \frac{1}{1-\alpha}\ln \sum_{i=Th_1}^{Th_2-1}\left(\frac{h_i}{w_0}\right)^{\alpha}, w_1 = \sum_{i=Th_1}^{Th_2-1} h_i,\\
E_{R2} &= \frac{1}{1-\alpha}\ln \sum_{i=Th_2}^{Th_3-1}\left(\frac{h_i}{w_0}\right)^{\alpha}, w_2 = \sum_{i=Th_2}^{Th_3-1} h_i,\\
E_{Rn} &= \frac{1}{1-\alpha}\ln \sum_{i=Th_n}^{L-1}\left(\frac{h_i}{w_0}\right)^{\alpha}, w_3 = \sum_{i=Th_n}^{L-1} h_i.
\end{aligned} \tag{14}$$

3.2 Electromagnetism-like mechanism

Electromagnetism-like mechanism optimization (EMO) is an evolutionary method having grounds on population. Initially, Birbil et al. [17] introduced the EMO algorithm to solve the problems related to unconfined optimization. Unlike other evolutionary optimization methodologies, EMO shows fast convergence and keeps its ability to avoid local minima in the presence of high modality surroundings [24]. Many researchers [18] have revealed that the EMO algorithm provides the superlative balance between the demand for evaluation of functions and the results from optimization. The EMO method is designed to crack the problem of searching for a global solution. When implementing EMO, it uses N number of n-dimensional points $x_{i,\ t}$ where, $i = 1, 2,\ldots,n$ and t defines the number of generation (or iteration) used in the algorithm. To search the feasible set in the n-dimensional points can be formulated by Eq. (15):

$$X = \{x \in R^n | l_i \le x \le u_i\}. \tag{15}$$

The initial population is expressed by using $S_{p,\ t} = \{x_{1,\ t}, x_{2,\ t}, \ldots, x_{N,\ t}\}$. When the value of t is taken as 1, it shows that the samples in the search region X are distributed uniformly. $S_{p,t}$ denotes the population class at t_{th} iteration and as the value of t changes the members of $S_{p,t}$ varies. After $S_{p,t}$ is initialized, an EMO algorithm will continue its looping process until a halting criterion such as the maximum number of iterations is encountered. EMO's iteration mainly comprises two steps: firstly, each point in the initial population travels to a different position on the basis of attraction-repulsion mechanism. In the second step, electromagnetic an attraction-repulsion principle moves the points which are further agitated locally by a search which makes them the members of $S_{pt+\ 1}$ in the iteration $t+\ 1_{th}$. The local search of EMO and the electromagnetism principle drive the members $S_{p,t}$ and $x_{i,t}$ closest to the optimal value.

Concerning the theory of the electromagnetics related to charged particles, each in the search space X is considered a charged particle and on the basis of fitness function's value, where the charge of a point is calculated. The charge obtained for a point is directly proportional to the objective (or fitness) function value. The principle of attraction-repulsion technique defines that the points with more charge attract others, whereas the points with lesser charge repel others. At last, a sum of total force vector $F_{i,t}$ which is exerted on a point can be evaluated by adding the attraction-repulsion forces, and each $x_{i,t}$ that belongs to $S_{p,t}$ is moved in the direction of its total force to the location $y_{i,t}$. A localized search is used to browse the surroundings of each and every particle in accordance with its objective value. The members, $x_{i,\ t+1}$ belonging to $S_{p,t}$, of $t+\ 1_{th}$ iteration are searched by the use of Eq. (16):

$$x_{i,t+1} = \begin{cases} y_{i,t}; f\left(y_{i,t}\right) \le f\left(z_{i,t}\right) \\ z_{i,t}; else \end{cases}. \tag{16}$$

The pseudo algorithm for EMO is given below as:

Algorithm EMO ($iter_{max}$, $iter_{local}$, δ, N)

1. *Input parameters*: Iteration'sup *per*lim*it* $\left(iter_{max}\right)$, *parameter for local* search$\left(iter_{local}\right)$, *Minimum distance* (δ), *size* of population(N).
2. *Initialization*: *The counter for iteration is set at* $t\ =1$, *While maintaining the uniformity in* X, *initialize the number of* Sp_i *and detect the best point in* Sp_i.
3. *While* $t < iter_{max}$ *do*
4. $F_i \leftarrow CalculateF\left(Sp_t\right)$
5. $Y_{i,\ t} \leftarrow move\ \left(x_{i,\ t}, F_i\right)$
6. $z_{i,\ t} \leftarrow local\ \left(iter_{local}, \delta, y_{i,\ t}\right)$
7. $x_{i,\ t+1} \leftarrow Select\ \left(Sp_{t+1}, y_{i,\ t}, z_{i,\ t}\right)$

End while.

In addition, the detail steps of the proposed EMO based multilevel thresholding scheme have been also offered. The following are the steps involved in the implementation of electromagnetism-like mechanism optimization (EMO) algorithm:

Step 1: Define the input parameters: Initialize the maximum length of iterations $iter_{max}$. In case of local search stage, $n \times iter_{local}$ gives the $z_{i,t}$ which is representing the maximum number of positions, within the δ distance of $y_{i,t}$, for each dimension i.

Step 2: Initialize: Select the (points) $x_{i,\ t}$, at $t=1$ uniformly in X, i.e., $x_{i,\ 1} \approx Unif\ (X)$, I = 1, 2,...,N, where *Unif* is representing the uniform distribution. Compute the fitness function values $f\ (x_{i,\ t})$ and identify the best point for minimization and maximization, which can be done using Eqs. (17) and (18):

$$x_t = \arg \min_{X_{i,t} \in S_t} \left\{ f\left(x_{i,t}\right) \right\} \tag{17}$$

and

$$x_t = \arg \max_{X_{i,t} \in S_t} \left\{ f\left(x_{i,t}\right) \right\}. \tag{18}$$

Step 3: Calculate the force after assigning a charge like value ($q_{i,t}$) to each and every point ($x_{i,t}$). The charge $q_{i,t}$ has a dependency on $f(x_{i,t})$ which implies that, if a point has more charge, it has a better fitness value. Use Eq. (19) to compute the charge:

$$q_{i,t} = \exp\left\{ -n \frac{f(x_{i,t}) - f(x_t)}{\sum_{j=1}^{N} f(x_{i,t}) - f(x_t)} \right\}. \tag{19}$$

Step 4: For each t, determine the force between i_{th} point $x_{i,t}$ and j_{th} point $x_{j,t}$ using the equation given as:

$$F_{i,\mathrm{j}} = \begin{cases} (x_{j,t} - x_{i,t}) \dfrac{q_{j,t} \cdot q_{i,t}}{\left\| x_{j,t} - x_{i,t} \right\|^2}; f(x_{j,t}) < f(x_{i,t}) \\ (x_{i,t} - x_{j,t}) \dfrac{q_{j,t} \cdot q_{i,t}}{\left\| x_{j,t} - x_{i,t} \right\|^2}; f(x_{j,t}) \geq f(x_{i,t}) \end{cases} \tag{20}$$

and calculate the total force for each t as:

$$F_i = \sum_{j=1, j \neq i}^{N} F_{i,\mathrm{j}}. \tag{21}$$

Step 5: Except x_t, each point $x_{i,t}$ is to be moved along F_i utilizing the Eq. (22)

$$x_{i,t} = x_{i,t} + \lambda \frac{F_i}{\| F_i \|}(RNG), i = 1, 2, \ldots, N, \tag{22}$$

where, $\lambda \approx Unif(0, 1)$ for each and every point $x_{i,t}$ and the allowable movement range towards the upper and lower bound for a respective dimension is defined by RNG.

Step 6: For each $y_{i,t}$, generate a maximum of $iter_{local}$ points for every direction of coordinate which should remain in the δ neighborhood of $y_{i,t}$. Continue the process until either a better $z_{i,t}$ is obtained or the iteration reaches its maximum value i.e., $n \times iter_{local}$.

Step 7: For the selection of the next iteration $x_{i,t+1}$, which belongs to S_{pt+1} are selected from $z_{i,t}$ and $y_{i,t}$ using Eq. (16) to identify the extreme point using Eq. (17) for minimization or Eq. (18) for maximization.

The aim of this paper is to maximize the Renyi's objective (or fitness) function using electromagnetism-like mechanism optimization (EMO). A complete systematic flowchart routine of the proposed EMO-Renyi's based multilevel color image thresholding is shown in the Fig. 2.

4 Experiment results and discussion

In this section, experiment outcomes have been demonstrated to estimate and validate the performance of the proposed (EMO-R) methodology along with Kapur's and Tsallis based existing approaches using each optimization algorithm for normal as well as satellite images. In satellite images, different bands with different frequency regions make the algorithms inefficient and containing high resolution is an additional source of inadequacy. In satellite image segmentation, the presence of intrinsic uncertainty makes the search of interested

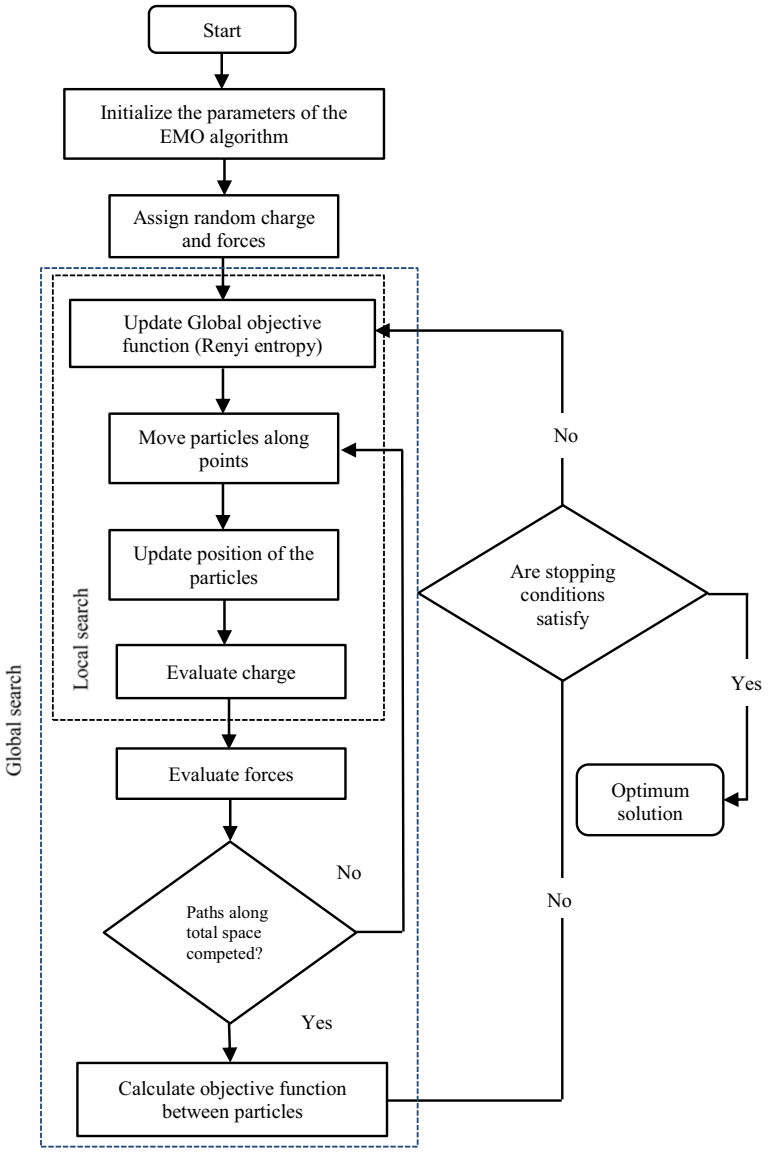

Fig. 2 Flowchart of the proposed EMO-R based multilevel thresholding scheme

domain imprecise. Multi-level thresholding can be used for efficient satellite image segmentation. Therefore, in this paper, optimizing techniques with Kapur's, Tsallis, and Renyi's entropy as an objective function has been presented towards accurate and fast multilevel based segmentation for daily-life and satellite images.

4.1 Image dataset

With a view to obtaining a better estimation of the segmented output of the proposed (EMO-R) scheme, the performance of Kapur's and Tsallis entropies are compared using each optimization algorithm. Therefore, experimental results of each selected methods such as BAT, BSA, FA, PSO, WDO, and EMO algorithm with Kapur's entropy, Renyi's entropy, and Tsallis entropy have been shown separately. Moreover, for better discrimination of each method, the trials have been steered on 10 entirely diverse images with distinct histogram characteristic. To check the robustness of the proposed (EMO-R) scheme for different feature images, the first five test images are included as well-known standard color images and the next five are considered as high-resolution satellite images which are shown in Fig. 3(1–10). Each of the images depicts a histogram which is exclusive in itself which is indicated in Fig. 3(1′-10′). All the 10 images have diverse features that add on to the result of the segmented image.

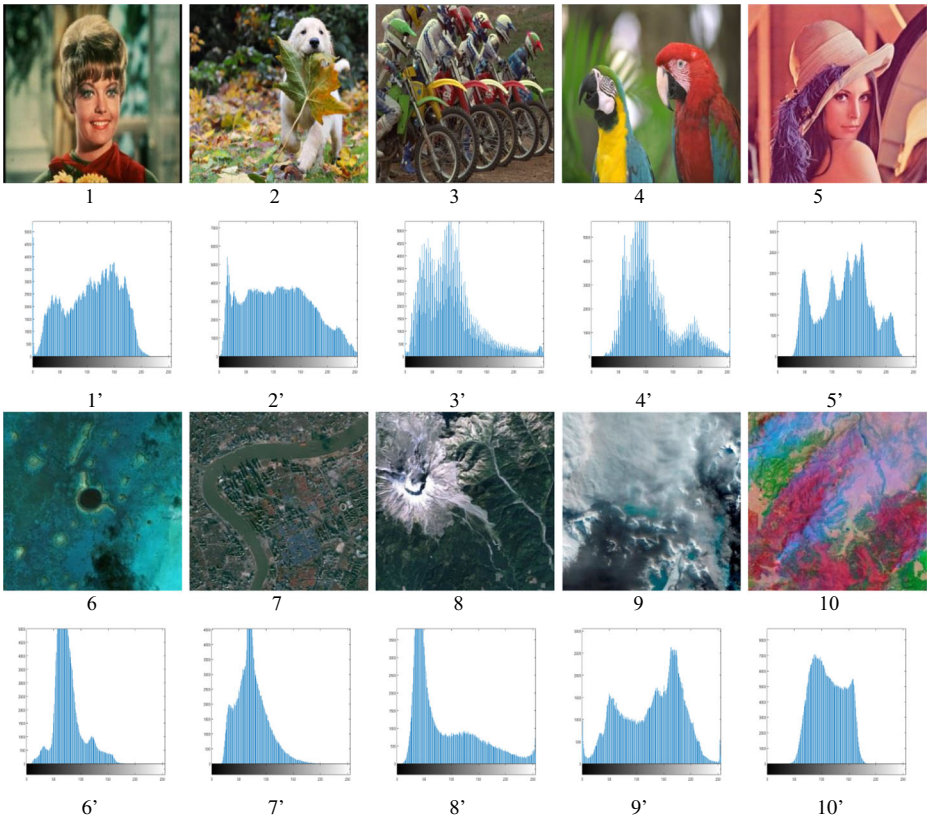

Fig. 3 Images (1–10) depict standard and satellite test images, (1′-10′) represent respective histogram images

4.2 Measurement parameters to assess image quality

This section represents different prominent fidelity factors such as structural-similarity index (SSIM) and feature-similarity index (FSIM), misclassification error (ME), mean-squared error (MSE) and peak signal-to-noise ratio (PSNR), which have been utilized to show the quality of the proposed and compared methods. The image fidelity parameters like mean error (ME), mean squared error (MSE), peak signal to noise ratio (PSNR), structural similarity index module (SSIM), feature similarity index module (FSIM) and Entropy values are taken to test the efficiency of the proposed method.

These parameters are used to represent the quality of the segmented image. MSE calculates the difference between the expected value and actual value. PSNR is used to calculate the peak signal to noise ratio between original and segmented image. SSIM is the structural similarity index needed to calculate the structural similarity and FSIM used to evaluate the feature similarity of the segmented and original image. Higher values of SSIM and FSIM indicate higher performance. The formulae for all these parameters are defined in Table 1. The values of important parameters of each of the optimization algorithm are presented in Table 2. The determination of the proper value of the entropic parameter is important. The parameter q and α represents the variable for Tsallis and Renyi's entropy respectively. The value of q is fixed at 0.8, which is an endorsed value in literature such as [50]. The optimum value for α and q is set after several experiments. The value of α is set to 0.8 and the value of q is also set to 0.8. The values of α beyond 1 give poor results. When q is set from 0.5 to 0.9 the same results are obtained. The optimum results are obtained, when α is 0.8.

4.3 Performance evaluation and comparison

The simulation results are arranged in the form of separate tables and invisulats graphical plots for each parameter to examine a different aspect of the thresholded images. To evaluate the overall performance different parameters are examined which are shown quantitatively in Tables 3, 4, 5, 6, 7, 8, 9, 10, and 11. Furthermore, CPU time (in seconds) is computed in Table 12, to estimate the computational difficulties or efficiency of the proposed EMO-R approach.

Table 1 Different metrice to test the efficiency of each methods

S. No.	Parameters	Formula	Remarks
1.	Misclassification error (ME) [37]	$ME = 1 - \frac{\lvert B_O \cap B_T \rvert + \lvert F_O \cap F_T \rvert}{\lvert B_O \rvert + \lvert F_O \rvert}$	Calculates the mean error between segmented and an original image.
2.	Mean Square Error (MSE) [9]	$MSE = \sqrt{\frac{\sum_{i=1}^{J}\sum_{j=1}^{K}\left(I(\mathrm{i,j}) - \mathrm{I}'(\mathrm{i,j})\right)^2}{JK}}$	Calculates the difference between expected value and the actual value.
3.	Peak Signal to Noise Ratio (PSNR) [11]	$PSNR(\text{in dB}) = 20\log_{10}(255/MSE)$	It is the ratio of the maximum power of a signal to the power of noise.
4.	Structural Similarity Index (SSIM) [8]	$SSIM\left(\mathrm{I}, \mathrm{I}'\right) = \frac{\left(2\mu_I\mu_{I'} + l_1\right)\left(2\sigma_{II'} + l_2\right)}{\left(\mu_I^2 + \mu_{I'}^2 + l_1\right)\left(\sigma_I^2 + \sigma_{I'}^2 + l_2\right)}$	Evaluates the similarity between the segmented image and an original image.
5.	Feature Similarity Index (FSIM) [8]	$FSIM = \frac{\sum_{c=1}^{N} S_D(c) PC_{\max}(\mathrm{c})}{\sum_{c=1}^{N} PC_{\max}(\mathrm{c})}$	Calculates the feature similarity of segmented and an original image.
6.	Entropy [46]	$Entropy = \sum_i P_i \log_2 P_i$	Indicates the information of an image.

Table 2 Parameters and their respective values used in optimization algorithms

Algorithms	Parameters	Values
BAT	Frequency max (Q_{max})	0.2
	Frequency min (Q_{min})	0
	Loudness (A)	1
	Microbats frequency	50
	Pulse rate (R)	0.5
FA	Light absorption coefficient (γ)	1
	Inertial attractiveness (β_0)	1
	Number of fireflies (N)	50
	Number of generations (N_{gen})	100
	Randomization parameter (α)	0.5
PSO	Cognitive, social and neighborhood acceleration (C_1, C_2, C_3)	2, 2, 1
	Error goal and max trial limit	1e-7 & 500
	Lower bound lb (W_{min}) and Upper bound ub (W_{max})	1 & 256
	Maximum velocity step, constriction factor and neighborhood size	1
	No. of Iterations	1000
	Swarm size	200
	The fraction of maximum iterations, for which W is linearly varied	0.7
	Value of global minima	0
	Value of velocity weight at the beginning	0.95
	Value of velocity weight at the end of the PSO iterations	0.4
WDO	Constant in the update equation	0.5
	Coriolis effect coefficient (c)	0.4
	Gravitational constant (g)	0.2
	Maximum allowed speed or velocity limit	0.3
	Maximum no. of iteration	500
	Population size	20
	RT coefficient	2
EMO	Maximum number of iteration ($Iter_{max}$)	150
	Local search parameter ($Iter_{local}$)	10
	Minimum distance (δ)	0.025
	Population size (N)	50

Figures 4, 5, 6, 7, 8, 9, 10, and 11 visually evaluate the overall segmented results and illustrate the pictorial view demonstration of thresholded images. The proposed method has been shown the best-segmented images in a thorough examination of the qualitative evaluation part. A comparison with other nature-inspired optimization algorithms (BAT, BSA, FA, PSO, and WDO) are incorporated using Kapur's, Tsallis, and Renyi's entropy at 3, 5, 8 and 16 levels of threshold, to adjudicate the performance of the proposed EMO-Renyi's scheme. However, among all methods, EMO-Renyi's based approach is superior, but BAT, BSA, FA, PSO, and WDO are also producing satisfactory results with Renyi's entropy.

Figures 12, 13, 14, 15, 16, 17, 18, 19, 20, 21, 22, 23, 24, 25, 26, 27, 28, and 29 depict the graphical plots of numerical parameters together, whereas Figs. 12, 13, 14, 15, 16, 17, 18, 19, 20, 21, 22, 23, 24, 25, 26, 27, 28, and 29 report the comparison plots of ME, MSE, PSNR, SSIM, FSIM, and CPU time using Kapur's Tsallis and Renyi's entropy for 8-level of threshold using BAT, BSA, FA, PSO, WDO, and EMO correspondingly. Figures 30 and 31 represent the computational efficiency of the proposed scheme for a different level of threshold. To test the effectiveness, efficiency, and robustness of the proposed EMO and Renyi based algorithm, three different objective (or fitness) functions are examined. They are presented separately as follows:

Table 3 Comparison of ME and best objective values (entropy) computed by different algorithm using Kapur's entropy

Test images	M	ME						Best objective values					
		BAT	BSA	FA	PSO	WDO	EMO	BAT	BSA	FA	PSO	WDO	EMO
1	3	0.0853	0.1179	0.1179	0.1179	0.1252	0.1217	15.4688	15.5161	15.5161	15.5161	15.5161	15.5143
	5	0.0718	0.0752	0.0752	0.0751	0.0784	0.0718	20.0571	21.0600	21.0600	21.0584	21.0598	21.0580
	8	0.0364	0.0390	0.0390	0.0442	0.0519	0.0273	27.9837	28.1977	28.1947	28.0810	28.1825	28.0432
	16	0.0197	0.0213	0.0197	0.0212	0.0546	0.0194	39.4717	42.9030	40.8391	41.4743	42.0711	42.5375
2	3	0.3298	0.2471	0.2471	0.2471	0.2471	0.2433	16.2735	16.3874	16.3874	16.3874	16.3874	16.3873
	5	0.2277	0.1684	0.1684	0.1614	0.1718	0.1718	21.8630	22.1723	22.1723	22.1697	22.1717	22.1700
	8	0.1371	0.1234	0.1196	0.1405	0.1371	0.1137	29.1735	29.7063	29.7027	29.6818	29.6937	29.6778
	16	0.0086	0.0646	0.0548	0.0939	0.0732	0.0548	43.3646	45.4416	45.4121	44.4538	45.3852	45.0768
3	3	0.2332	0.2632	0.2632	0.2883	0.2632	0.2632	16.1352	16.1680	16.1680	16.1650	16.1680	16.1680
	5	0.2942	0.2221	0.1669	0.1370	0.2278	0.1370	21.5648	21.9206	21.8967	21.8999	21.9206	21.8941
	8	0.0746	0.0418	0.0418	0.0459	0.1294	0.0418	28.8712	29.3904	29.3832	29.3355	29.3244	29.3350
	16	0.0037	0.0013	0.0013	0.0022	0.0011	0.0079	43.1392	45.3287	45.2944	44.1996	45.1337	44.1901
4	3	0.4611	0.1400	0.1619	0.1400	0.1400	0.1319	15.3741	15.5576	15.5562	15.5576	15.5576	15.5562
	5	0.0061	0.0034	0.0203	0.0203	0.0026	0.0203	20.8516	21.2378	21.2240	21.2157	21.2178	21.1944
	8	0.0019	0.0034	0.0034	0.0033	0.0061	0.0034	28.1573	28.6871	28.6060	28.6045	28.6111	28.6275
	16	0.0017	0.0034	0.0019	0.0019	0.0047	0.0034	41.4782	43.7499	43.4736	42.3231	43.0812	43.1084
5	3	0.0219	0.0219	0.0219	0.0219	0.0257	0.0189	15.2932	15.3183	15.3183	15.3183	15.3183	15.3160
	5	0.0014	1.90e-04	1.90e-04	1.18e-04	0.0004	1.01e-04	20.2760	20.6095	20.6095	20.5957	20.6093	20.5763
	8	1.90e-04	0	0	0	0	6.86e-05	25.9690	27.3190	27.3031	27.2054	27.3047	27.2793
	16	0	0	0	0	0	0	36.0107	41.7892	39.9509	40.2743	41.4205	41.4954
6	3	0.0386	0.0394	0.0394	0.0393	0.4408	0.0382	14.6105	14.6857	14.6857	14.6857	14.4378	14.6783
	5	0.0314	0.0394	0.0394	0.0393	0.0381	0.0394	20.0116	20.3187	20.3180	20.3150	20.2738	20.1376
	8	0.0057	0.0057	0.0065	0.0082	0.0406	0.0155	26.4627	27.2750	27.2705	27.1691	27.0853	26.8405
	16	7.40e-04	0.0038	0.0038	0.0043	0.00577	0.0057	37.6717	41.4708	39.6979	40.1946	41.1964	40.9721
7	3	0.5695	0.7984	0.7905	0.6845	0.6957	0.6846	15.1444	15.2164	15.2108	15.2094	15.2094	15.2094
	5	0.0991	0.1851	0.1950	0.1850	0.1567	0.1950	20.3123	21.0503	21.0501	21.0427	21.0416	21.0391
	8	0	0.1394	0.0835	0.1228	0.0834	0.0670	26.2603	28.3493	28.2242	28.1114	28.2131	28.2071
	16	3.81e-06	0.0169	0.0057	0.0505	0.0168	7.05e-04	40.4381	43.3261	43.2470	42.2980	42.9178	42.5155
8	3	0.6275	0.5410	0.5410	0.5410	0.5468	0.5410	15.9611	16.0874	16.0874	16.0874	16.0874	16.0874
	5	0.0016	0.4437	0.4437	0.4437	0.4650	0.4312	20.6857	21.8095	21.8095	21.8095	21.8095	21.8036
	8	7.60e-05	0.3143	0.0079	0.2290	0.3344	0.3143	27.8949	29.1095	29.0240	29.0624	29.0997	29.0607

Table 3 (continued)

Test images	M	ME						Best objective values					
		BAT	BSA	FA	PSO	WDO	EMO	BAT	BSA	FA	PSO	WDO	EMO
	16	0.0079	3.60e-05	1.56e-04	3.60e-05	0.0001	1.36e-04	43.0601	44.8727	44.8447	44.0703	44.4408	44.7181
9	3	0.0410	0.0410	0.1526	0.0409	0.1450	0.1563	15.9008	15.9999	15.9987	15.9990	15.9987	15.9983
	5	0.0330	0.0350	0.0350	0.0368	0.0330	0.0329	21.6860	22.0190	21.9915	22.0169	21.9918	22.0185
	8	0.0128	0.0113	0.0137	0.0163	0.0153	0.0154	29.4203	29.6585	29.6355	29.5892	29.6415	29.5646
	16	0.0237	0.0080	0.0086	0.0103	0.01194	0.0062	43.7338	45.3418	45.1840	44.5965	44.8733	45.0081
10	3	5.54e-05	5.54e-05	5.54e-05	5.54e-05	5.54e-05	5.54e-05	14.2501	14.3493	14.3493	14.3493	14.3490	14.3493
	5	4.84e-05	5.54e-05	5.54e-05	5.54e-05	5.54e-05	4.54e-05	18.7150	19.5904	19.5850	19.5889	19.4651	19.5284
	8	5.54e-05	5.36e-05	5.54e-05	5.36e-05	5.54e-05	4.54e-05	22.0633	26.3417	26.3147	26.2067	26.2787	26.2982
	16	4.51e-05	3.63e-05	2.94e-05	5.19e-05	5.36e-05	4.15e-05	36.7045	40.6658	38.9237	37.7941	39.8464	40.3968

Table 4 Comparison of ME and best objective values (entropy) computed by different algorithm using Tsallis entropy

Test images	M	ME						Best objective values					
		BAT	BSA	FA	PSO	WDO	EMO	BAT	BSA	FA	PSO	WDO	EMO
1	3	0.0129	0.0085	0.0085	0.0084	0.0129	0.0082	24.5801	4762.0167	4761.8321	4762.0167	4762.0167	4762.0167
	5	0.0163	0.0085	0.0085	0.0084	0.0124	0.0082	32.0213	4769.6707	4769.4077	4769.6705	4769.6472	4769.4073
	8	0.0123	0.0085	0.0085	0.0084	0.0124	0.0082	39.0427	4778.9818	4778.3267	4778.9409	4778.8589	4778.9238
	16	0.0085	0.0085	0.0085	0.0084	0.0126	0.0082	4785.32204	4796.5647	4796.3324	4794.4529	4793.4690	4795.6398
2	3	0.2110	0.2471	0.2471	0.2471	0.2510	0.2471	25.1810	25.4464	25.4464	25.4464	25.4464	25.4463
	5	0.1031	0.1684	0.1684	0.1683	0.1755	0.1684	32.2038	32.9062	32.9062	32.9037	32.9025	32.9062
	8	0.1337	0.1234	0.1157	0.1116	0.1304	0.1034	41.6557	42.1757	42.1630	42.1491	42.1724	42.1737
	16	0.0375	0.0646	0.0548	0.0732	0.0374	0.0120	58.5425	60.1876	60.1436	58.8965	59.8522	59.7441
3	3	1.16e-04	8.13e-05	1.16e-04	8.15e-05	8.13e-05	4.13e-05	33.0218	1092.4528	33.0523	1029.4502	1092.4488	1092.4502
	5	1.16e-04	8.13e-05	8.13 e-04	8.13e-05	0.0001	4.13e-05	40.2530	1100.7821	1100.7514	1100.7773	1100.7798	1100.7762
	8	4.98e-04	8.13e-05	8.13 e-04	8.13e-05	8.13e-05	4.13e-05	45.13055	1110.5672	1110.1531	1110.4981	1110.3046	1110.4534
	16	8.13e-05	8.13e-05	8.13 e-04	8.13e-05	0.0001	4.13e-05	1124.0342	1129.4631	1129.1595	1126.8199	1128.1135	1129.0895
4	3	0	0	0	0	0	0	1030.9147	1031.4531	1031.4531	1031.4531	1031.4531	1031.4531
	5	0	0	0	0	0	0	1034.4312	1039.2416	1039.2037	1031.4531	1039.2039	1039.2291
	8	0	0	0	0	0	0	1046.9207	1049.0320	1049.0320	1048.9783	1048.9887	1049.0019
	16	0	0	0	0	0	0	1063.1281	1067.2403	1066.9231	1065.4631	1066.6233	1066.6184
5	3	0.0219	0.0189	0.0189	0.0189	0.0189	0.0158	23.1241	23.144594	23.1454	23.1454	23.1454	23.1448
	5	0.0043	1.90e-04	1.90 e-04	3.01 e-04	0.0003	1.18e-04	29.4866	29.784391	29.7843	29.7715	29.7816	29.6990
	8	3.01e-04	0	0	0	0	0	36.2360	37.8586	37.8380	37.7079	37.6293	37.7194
	16	0	0	0	0	0	0	50.5108	54.3639	54.2588	53.2031	53.9174	53.7331
6	3	0.0382	0.0407	0.0407	0.0406	0.0406	0.0378	21.8091	22.0251	22.0251	22.0251	21.5547	22.0251
	5	0.0394	0.0394	0.0394	0.0393	0.0406	0.0407	28.8523	29.3873	29.0175	29.3777	29.3873	29.0216
	8	0.0021	0.0057	0.0074	0.0418	0.0093	0.0057	36.6318	37.7902	37.6690	37.2898	37.7486	37.7795
	16	0.0038	0.0043	0.0038	0.0031	0.0155	0.0011	45.3094	53.6917	53.3472	25.1825	52.8783	52.7605
7	3	0.5964	0.7984	0.7170	0.6845	0.7466	0.7466	22.9946	23.1607	23.1251	23.1277	23.1287	23.1287
	5	0.3009	0.1851	0.1950	0.2053	0.1851	0.1850	29.8691	30.7784	30.7653	30.7555	30.7777	30.7784
	8	0.1394	0.1394	0.1394	0.1468	0.1567	0.1378	38.0586	39.7212	39.7181	39.4169	39.5038	39.6063
	16	9.15e-05	0.0124	7.05 e-04	0.0123	0.0353	3.70 e-05	53.6313	56.7064	56.6008	55.3601	56.4674	56.0017
8	3	0.5158	8.00e-06	0.5291	8.00e-06	0.5411	8.00e-06	24.7687	25.4172	24.8434	25.4166	24.8434	25.4172
	5	0.3707	8.00e-06	0.4437	8.00e-06	0.4748	8.00e-06	31.9273	33.7308	32.1937	33.7224	32.1937	33.5658
	8	3.32e-04	8.00e-06	8.00e-06	8.00e-06	0.0062	8.00e-06	38.9359	43.3141	42.3533	43.2397	41.0945	43.3116

Table 4 (continued)

Test images	M	ME						Best objective values					
		BAT	BSA	FA	PSO	WDO	EMO	BAT	BSA	FA	PSO	WDO	EMO
	16	1.20e-05	8.00e-06	1.56e-04	8.00e-06	8.00e-06	8.00e-06	59.0626	62.4500	59.2559	61.4784	61.7616	62.3417
9	3	0.0090	0.0020	0.0369	0.0019	0.0394	0.0369	24.5663	879.7134	24.9116	879.7134	24.9101	24.9101
	5	0.0369	0.0020	0.0020	0.0019	0.0082	0.0010	32.2850	888.2831	887.8755	888.2831	888.1106	888.2831
	8	0.0016	0.0020	0.0020	0.0019	0.0058	0.0010	41.3181	898.5178	896.9144	898.4685	898.3525	898.4870
	16	0.0020	0.0020	0.0020	0.0019	0.0019	0.0010	912.4885	917.4089	917.3363	916.2366	915.7350	916.9988
10	3	5.36e-05	6.92e-06	6.92e-06	6.92e-06	5.54e-05	6.90e-06	20.6058	24.3975	23.1416	24.3975	21.2887	24.3973
	5	4.84e-05	6.92e-06	6.92e-06	6.92e-06	5.54e-05	6.90e-06	27.3315	31.7419	29.0708	31.7419	28.1553	31.4731
	8	3.46e-05	6.92e-06	6.92e-06	6.92e-06	5.54e-05	6.90e-06	33.9877	40.6020	40.4541	40.4653	36.3633	40.5945
	16	2.94e-05	6.92e-06	6.92e-06	6.92e-06	6.92e-06	6.90e-06	49.0554	57.6650	50.6182	55.4894	54.9807	57.4230

Table 5 Comparison of ME and best objective values (entropy) computed by different algorithm using Renyi entropy

Test images	M	ME						Best objective values					
		BAT	BSA	FA	PSO	WDO	EMO	BAT	BSA	FA	PSO	WDO	EMO
1	3	0.0124	0.0084	0.0084	0.0084	0.0129	0.0129	16.0026	46.6879	46.6840	46.6879	46.6879	**16.1758**
	5	0.0155	0.0084	0.0084	0.0084	0.0132	0.0129	21.5777	52.5179	52.4377	52.4596	52.5040	**21.9781**
	8	0.0084	0.0084	0.0084	0.0084	0.0143	0.0084	56.5134	60.0881	59.9420	60.0405	59.2393	**60.0820**
	16	0.0162	0.0084	0.0084	0.0084	0.0110	0.0084	40.3980	75.4127	75.3721	73.6727	73.8172	**75.1135**
2	3	0.2716	0.2471	0.2471	0.2471	0.2471	0.2316	16.3930	16.4160	16.4160	16.4160	16.4159	**16.4129**
	5	0.1830	0.1684	0.1984	0.1718	0.1718	0.1656	22.0814	22.2132	22.2132	22.2116	22.2117	**22.2096**
	8	0.1508	0.1196	0.1234	0.1116	0.1304	0.1304	28.9992	29.7528	29.7528	29.6741	29.7511	**29.7347**
	16	8.21 e-04	0.0646	0.0733	0.0985	0.0811	0.0646	43.9093	45.5041	45.2728	44.6214	45.4579	**45.2169**
3	3	7.47 e-04	8.13e-05	8.13 e-05	8.13 e-05	0.0004	7.85 e-05	16.4161	39.8420	39.5303	39.8420	39.8420	**39.8390**
	5	6.94 e-04	8.13 e-05	8.13 e-05	8.13 e-05	0.2153	7.85 e-05	22.8005	46.1070	46.0825	46.1070	22.0222	**46.0979**
	8	8.13e-05	8.13 e-05	8.13 e-05	8.13 e-05	0.0004	7.85 e-05	53.2748	53.9679	53.5507	53.9364	53.9094	**53.8838**
	16	1.16 e-04	8.13 e-05	8.13 e-05	8.13 e-05	0.0004	7.85 e-05	48.1541	70.2736	69.9782	69.4864	69.1392	**69.8352**
4	3	0	0	0	0	0	0	38.8017	39.0991	39.0991	39.0991	39.0991	**39.0991**
	5	0	0	0	0	0	0	44.6611	45.0516	45.0516	45.0437	45.0435	**45.0190**
	8	0	0	0	0	0	0	52.4422	52.8516	52.8205	52.7895	52.6766	**52.7672**
	16	0	0	0	0	7.62 e-06	0	64.2317	68.6136	68.2877	67.2429	67.5290	**68.4520**
5	3	6.86e-05	0.0189	0.0219	0.0189	0.0257	0.0189	15.1557	15.3762	15.3760	15.3762	15.3760	**15.3762**
	5	0	1.90 e-04	3.01 e-04	4.38 e-04	0.0003	3.01 e-04	19.9782	20.6841	20.6840	20.6799	20.6806	**20.6840**
	8	0	0	0	0	2.28 e-05	0	26.9984	27.4435	27.4419	27.2783	27.4056	**27.3862**
	16	0	0	0	0	0	0	159.3850	41.9729	41.9740	40.4711	41.5528	**41.1509**
6	3	0.0419	0.0419	0.0432	0.0432	0.0432	0.0407	14.7824	14.8038	14.8038	14.8038	14.8038	**14.7363**
	5	0.0394	0.0394	0.0394	0.0393	0.0406	0.0394	19.7832	20.4333	20.4333	20.3768	20.2920	**20.4036**
	8	0.0065	0.0074	0.0074	0.0065	0.0393	0.0050	26.5103	27.4143	27.4084	27.2414	27.2150	**27.2450**
	16	0	0.0038	0.0050	0.0043	0.0093	0.0050	162.9108	41.6067	41.3977	40.5922	41.4462	**41.3401**
7	3	0.5695	0.6604	0.6604	0.6603	0.6603	0.7650	15.2258	15.3619	15.3619	15.3619	15.3619	**15.3581**
	5	0.2623	0.1851	0.2160	0.1949	0.2382	0.2160	21.0204	21.1799	21.1660	21.1699	21.1796	**21.1596**
	8	0.0353	0.1314	0.1068	0.0914	0.1068	0.0991	27.9937	28.4559	28.3980	28.3296	28.3460	**28.3642**
	16	0	0.0124	0.0085	0.0022	0.0003	0.0085	41.2746	43.4326	43.2913	42.3937	40.0963	**42.6599**
8	3	0.5468	8.00 e-06	0.5468	8.00 e-06	0.5468	0.5468	16.1360	16.3451	16.1443	16.3451	16.1443	**16.1443**
	5	0.0016	8.00 e-06	0.4437	8.00 e-06	0.4650	0.4029	20.6436	22.5922	21.8712	22.5905	21.8694	**21.8315**
	8	1.56e-04	8.00 e-06	8.00 e-06	8.00 e-06	0.0079	0.0049	28.7264	30.3376	29.1251	30.2099	29.1375	**29.1325**

Table 5 (continued)

Test images	M	ME						Best objective values					
		BAT	BSA	FA	PSO	WDO	EMO	BAT	BSA	FA	PSO	WDO	EMO
	16	0.0049	8.00 e-06	8.00 e-06	8.00 e-06	0.0028	8.00 e-06	44.1701	46.7165	46.4455	45.8395	44.7123	**46.4680**
9	3	0.0388	0.0020	0.0369	0.0019	0.0410	0.0016	16.0904	38.5251	16.1470	38.5251	16.1470	**16.1228**
	5	0.0099	0.0020	0.0020	0.0019	0.0145	0.0016	21.7138	44.8816	44.6963	44.8816	44.8590	**22.2361**
	8	0.0020	0.0020	0.0020	0.0019	0.0020	0.0016	51.3324	52.9738	512,824	52.9558	92.5150	**52.9714**
	16	0.0163	0.0020	0.0020	0.0019	0.0020	0.0016	43.8520	69.2985	68.8624	67.8756	68.4643	**68.7882**
10	3	5.54e-05	6.92 e-06	5.54e-05	6.92 e-06	5.54 e-05	6.92 e-06	14.3798	15.8945	14.4951	15.8945	14.4951	**15.7830**
	5	5.19e-05	6.92 e-06	6.92 e-06	6.92 e-06	5.54 e-05	6.92 e-06	18.9528	21.5161	21.3329	21.5057	19.7884	**21.5161**
	8	6.92e-06	6.92 e-06	6.92 e-06	6.92 e-06	6.92 e-06	6.92 e-06	25.6974	28.6919	28.0751	28.6030	28.3715	**28.4615**
	16	4.15e-05	6.92 e-06	6.92 e-06	6.92 e-06	2.42 e-06	2.42e-06	355.0843	43.6740	154.2315	42.7679	42.1958	**42.9690**

Table 6 Comparison of MSE, and PSNR computed by different algorithm using Kapur's entropy

Test images	M	MSE						PSNR					
		BAT	BSA	FA	PSO	WDO	EMO	BAT	BSA	FA	PSO	WDO	EMO
1	3	22.4404	33.9504	33.9504	33.9503	36.3261	35.0089	34.6205	32.8224	32.8224	32.8223	32.5286	32.6890
	5	21.3792	21.6628	21.6628	21.8291	22.9591	20.7113	34.8309	34.7737	34.7737	34.7404	34.5212	34.9687
	8	9.5228	10.5928	10.5293	12.2924	15.9766	5.8311	38.3432	37.8807	37.9068	37.2344	36.0959	40.4733
	16	2.8903	3.7377	3.0681	3.6464	18.4563	8.1545	43.5214	42.4048	43.2620	42.5121	35.4693	39.0168
2	3	96.8626	66.1609	66.1609	66.1609	66.3304	65.0425	28.2692	29.9248	29.9248	29.9247	29.9136	29.9988
	5	60.3343	42.2032	42.2032	39.9798	43.3136	43.3124	30.3252	31.8773	31.8773	32.1123	31.7645	31.7647
	8	32.6536	29.0136	31.9315	34.1169	33.0135	27.9678	32.9915	33.5048	33.0886	32.8011	32.9438	33.6642
	16	0.5599	12.9802	10.3840	21.2053	15.2760	10.3589	50.6495	36.9980	37.9672	34.8663	36.2906	37.9777
3	3	76.6384	87.6085	87.6085	95.4863	87.6103	87.6085	29.2863	28.7053	28.7053	28.3313	28.7052	28.7053
	5	99.0889	76.5658	62.2433	53.3244	78.3911	54.1869	28.1706	29.2905	30.1899	30.8615	29.1881	30.7919
	8	29.8966	16.3925	16.4408	18.1287	53.8873	16.3476	33.3746	35.9843	35.2441	35.5471	30.8159	35.9963
	16	1.2292	0.0924	0.1491	0.4420	0.0763	1.8147	47.2346	58.4736	56.3955	51.6758	59.3028	45.5427
4	3	179.5268	87.9346	100.3779	87.9346	87.6373	100.3779	25.5895	28.6892	28.1144	28.6892	28.7039	28.1144
	5	8.8894	4.0542	27.3660	27.3917	3.1411	27.1263	38.6421	42.0518	33.7587	33.7546	43.1599	33.7969
	8	4.6956	4.8623	4.6264	4.7234	9.3175	1.8585	41.4139	41.2624	41.4784	41.3882	38.4377	45.4392
	16	4.9839	5.0290	2.0428	1.9969	8.1510	1.5239	41.1551	41.1160	45.0286	45.1271	39.0186	46.3013
5	3	84.2856	84.9703	84.9703	84.9703	87.5792	79.3892	28.8733	28.8381	28.8381	28.8381	28.7067	29.1332
	5	70.1315	49.2484	49.2484	44.2182	56.1018	52.1456	29.6717	31.2069	31.2069	31.6747	30.6410	30.9586
	8	47.5497	39.9464	41.9002	47.8898	39.2465	31.8318	31.3593	32.1160	31.9086	31.3284	32.1927	33.1021
	16	4.80e-04	23.9639	5.91e-04	25.3936	25.5284	25.8632	81.3125	34.3352	80.4129	34.0835	34.0605	34.0040
6	3	10.9542	11.4797	11.4797	11.4797	136.5465	10. 5104	37.7350	37.5315	37.5315	37.5314	26.7779	37. 9146
	5	14.0877	12.9366	13.2539	13.0627	11.9215	11.2505	36.6424	37.0126	36.9074	36.9704	37.3674	37.6191
	8	7.6467	3.5530	3.7566	4.6766	18.2509	2.9851	39.2960	42.6248	42.3829	41.4314	35.5179	43.3812
	16	7.3938	4.4227	3.6045	5.4044	8.3040	0.4999	39.4421	41.6739	42.5624	40.8032	38.9378	51.1421
7	3	151.0183	208.9164	206.9165	179.8280	183.0195	179.8280	26.3405	24.9311	24.9729	25.5822	25.5058	25.5822
	5	27.1022	50.0431	53.0934	50.0348	42.5803	52.4995	33.8008	31.1374	30.8804	31.1380	31.8387	30.9293
	8	0.0055	43.2374	26.2701	35.2862	26.4596	20.8912	70.6995	31.7722	33.9362	32.6547	33.9049	34.9312
	16	0.6862	6.9637	3.1843	19.3534	6.7407	1.2051	49.7664	39.7024	43.1006	35.2632	39.8437	47.3207
8	3	162.4864	139.3332	139.3330	139.3331	140.8207	139.3329	26.0226	26.6903	26.6903	26.6902	26.6441	26.6910
	5	1.8389	116.0839	116.0839	116.0839	121.5925	113.3859	45.4852	27.4831	27.4831	27.4830	27.2817	27.3859
	8	0.0241	91.7341	6.2814	72.2546	96.1318	0.0241	64.3142	28.5055	40.1502	29.5421	28.3021	64.3142

Table 6 (continued)

Test images	M	MSE						PSNR					
		BAT	BSA	FA	PSO	WDO	EMO	BAT	BSA	FA	PSO	WDO	EMO
	16	7.4991	0.0085	0.2662	0.0087	0.2073	0.4292	39.3807	68.8427	53.8794	68.6978	54.9630	51.8038
9	3	13.8641	13.7633	45.3782	13.7633	43.3914	46.2945	36.7119	36.7436	31.5623	36.7435	31.7567	31.4755
	5	11.7837	11.8565	11.9809	12.5418	11.2473	11.8565	37.4180	37.3912	37.3459	37.1471	37.6202	37.3912
	8	2.8407	4.3622	3.2791	5.1419	4.3868	1.9655	43.5965	41.7337	42.9733	41.0195	41.7092	45.1962
	16	9.7756	0.3823	0.5610	1.3323	2.3686	0.1343	38.2294	52.3070	50.6411	46.8827	44.3858	56.8490
10	3	1.8077	1.7698	1.7698	1.7698	2.2031	1.7698	45.5595	45.6515	45.6515	45.6514	44.7003	45.6515
	5	0.2763	3.8859	3.8424	3.7286	3.7254	2.3186	53.7170	42.2359	42.2848	42.4153	42.4190	44.4786
	8	3.0796	1.8068	3.6093	1.8969	3.5405	1.8068	43.2458	45.5617	42.5566	45.3501	42.6400	45.5617
	16	0.2793	0.0481	0.0102	2.1941	3.9312	0.0562	53.6705	61.3104	68.0437	44.7180	42.1855	60.6323

Table 7 Comparison of MSE, and PSNR computed by different algorithm using Tsallis entropy

Test images	M	MSE						PSNR					
		BAT	BSA	FA	PSO	WDO	EMO	BAT	BSA	FA	PSO	WDO	EMO
1	3	0.1097	0.0085	0.0085	0.0084	0.0860	0.0085	57.7281	68.8368	68.8368	68.8367	58.7832	68.8368
	5	0.7235	0.0085	0.0085	0.0084	0.0452	0.0085	49.5366	68.8368	68.8368	68.8367	61.5730	68.8368
	8	0.0348	0.0085	0.0085	0.0084	0.0463	0.0085	62.7167	68.8368	68.8368	68.8367	61.4674	68.8368
	16	0.0085	0.0085	0.0085	0.0084	0.0916	0.0085	68.8323	68.8368	68.8368	68.8367	58.5086	68.8368
2	3	54.8049	66.1609	66.1609	66.1609	67.6857	66.1612	30.7426	29.9248	29.9248	29.9247	29.8258	29.9248
	5	23.1866	42.2032	42.2032	42.2757	44.5814	42.2032	34.4784	42.2032	31.8773	31.8698	31.6392	31.8773
	8	32.6027	29.0136	26.8214	29.0010	31.1931	25.5196	32.9983	33.5048	33.8460	29.0010	33.1902	34.0620
	16	5.8999	12.9808	10.3883	15.1420	5.9288	0.9625	40.4224	36.9978	37.9654	36.3289	40.4010	48.2966
3	3	1.16e-04	8.13e-05	1.16e-04	8.13e-05	8.13e-05	8.13e-05	87.4495	89.0256	87.4495	89.0256	89.0256	89.0256
	5	1.22 e-04	8.13e-05	8.13 e-05	8.13e-05	0.0001	8.13e-05	87.2647	89.0256	89.0256	89.0256	87.2674	89.0256
	8	4.98 e-04	8.13 e-05	8.13 e-05	8.13e-05	8.13e-05	8.13e-05	76.6577	89.0256	89.0256	89.0256	89.0256	89.0256
	16	8.64 e-05	8.13 e-05	8.13 e-05	8.13e-05	0.0001	8.13e-05	88.7623	89.0256	89.0256	89.0256	86.1531	89.0256
4	3	4.06 e-05	2.28 e-05	2.59 e-04	2.54e-06	1.01e-05	1.60e-04	92.0359	94.5347	83.9911	104.0771	98.0565	86.0837
	5	2.54 e-06	3.81 e-05	2.54e-05	2.54e-06	4.57 e-05	1.52e-05	104.0771	92.3162	96.2956	104.0771	91.5243	96.2956
	8	1.47 e-04	2.28 e-05	3.53 e-04	1.27e-05	0.0003	5.08 e-06	86.4428	94.5347	82.6470	97.0874	82.1737	101.0668
	16	8.23 e-04	8.39 e-05	1.95 e-04	1.37e-04	0.0011	5.08e-06	78.9717	88.8920	85.2122	86.7539	77.5449	101.0668
5	3	83.0438	82.6362	82.6362	82.6362	82.6362	87.7044	28.9377	28.9591	28.9591	28.9590	28.9590	28.7006
	5	73.5709	49.2484	49.2484	51.3764	51.3067	46.8332	29.4637	31.2069	31.2069	31.0231	31.0290	31.4253
	8	56.9111	40.8777	38.6286	32.3708	26.1049	41.4488	30.5788	32.0159	32.2617	33.0292	33.9635	31.9557
	16	45.6648	23.9639	20.3860	25.6899	26.7409	18.5141	31.5350	34.3352	35.0375	34.0331	33.8590	35.4558
6	3	11.1353	11.5464	11.5464	11.5463	12.5968	11.5464	37.6638	37.5063	37.5063	37.5063	37.1281	37.5063
	5	14.6657	12.9366	14.0897	12.9680	13.3932	14.1312	36.4678	37.0126	36.6418	37.0020	36.8619	36.6290
	8	1.0365	3.5530	4.3742	19.1221	5.2383	3.2303	47.9752	42.6248	41.7218	35.3154	40.9388	43.0384
	16	4.0273	5.1834	4.0559	3.5698	14.5074	0.8255	42.0807	40.9847	42.0500	42.6043	36.5148	48.9638
7	3	156.0632	208.9164	187.6662	179.8280	196.0872	196.0873	26.1978	208.9164	25.3969	25.5822	25.2063	25.2063
	5	107.5226	50.0431	52.5064	55.4424	49.6848	50.0431	27.8158	50.0431	30.9287	30.6923	31.1685	31.1374
	8	48.6538	43.2344	43.2344	29.9861	53.6165	0.8981	31.2596	43.2344	31.7725	33.3616	30.8738	48.5976
	16	0.8682	5.3825	1.3322	5.4418	13.2519	0.8981	48.7444	40.8210	46.8852	40.7733	36.9080	48.5976
8	3	133.0125	5.20 e-05	136.3638	5.20 e-05	139.3359	5.20e-05	26.8919	90.9708	26.7383	90.9707	26.6901	90.9708
	5	100.2624	5.20 e-05	116.0839	5.20 e-05	124.1871	5.20e-05	28.1194	90.9708	27.4831	90.9707	27.1900	90.9708
	8	0.4274	5.20 e-05	5.20 e-05	5.20 e-05	5.0330	5.20e-05	51.8229	90.9708	90.9708	90.9707	41.1124	90.9708

Table 7 (continued)

Test images	M	MSE						PSNR					
		BAT	BSA	FA	PSO	WDO	EMO	BAT	BSA	FA	PSO	WDO	EMO
	16	0.0011	1.28 e-04	0.1691	1.80 e-04	0.0001	8.00e-05	77.6854	87.0587	55.8492	85.5780	86.5471	89.0999
9	3	0.2143	4.92e-04	12.2637	4.92e-04	11.5867	12.2681	54.8215	81.2103	37.2446	81.2103	37.4912	37.2430
	5	12.7200	4.92e-04	4.92e-04	4.92e-04	0.1809	4.92e-04	37.0859	81.2103	81.2103	81.2103	55.5553	81.2103
	8	0.0012	4.92e-04	4.92e-04	4.92e-04	0.0786	4.92e-04	77.4307	81.2103	81.2103	81.2103	59.1739	81.2103
	16	7.09e-04	4.92e-04	4.92e-04	5.30e-04	0.0004	4.92e-04	79.6211	81.2103	81.2103	80.8860	81.2103	81.2103
10	3	0.3247	1.73 e-06	1.73 e-06	1.73 e-06	2.1379	1.73e-06	53.0160	105.7471	105.7471	105.7470	44.8307	105.7471
	5	0.3790	1.73 e-06	1.73 e-06	1.73 e-06	4.0334	1.73e-06	52.3440	105.7471	105.7471	105.7470	42.0740	105.7471
	8	0.0112	1.73 e-06	3.46 e-06	3.46 e-06	5.3028	1.73e-06	67.6226	105.7471	102.7368	102.7367	40.8856	105.7471
	16	0.0047	1.73 e-06	1.73 e-06	1.73 e-06	8.82 e-05	1.73e-06	71.3648	105.7471	105.7471	105.7470	88.6713	105.7471

Table 8 Comparison MSE, and PSNR computed by different algorithm using Renyi entropy

Test images	M	MSE						PSNR					
		BAT	BSA	FA	PSO	WDO	EMO	BAT	BSA	FA	PSO	WDO	EMO
1	3	0.0393	0.0084	0.0084	0.0084	0.0784	0.0847	62.1844	68.8367	68.8367	68.8367	59.1844	**58.8477**
	5	0.5945	0.0084	0.0084	0.0084	0.1525	0.1057	50.3888	68.8367	68.8367	68.8367	56.2965	**57.8867**
	8	0.0084	0.0084	0.0084	0.0084	0.3529	0.0084	68.8367	68.8367	68.8367	68.8367	52.6532	**68.8367**
	16	101,946	0.0084	0.0084	0.0084	0.0127	0.0085	47.3582	68.8367	68.8367	68.8367	67.0875	**68.8345**
2	3	74.4854	66.1609	66.4609	66.1609	66.3244	61.1094	29.4101	29.9248	29.9248	29.9247	29.9140	**30.2697**
	5	47.1045	42.2032	42.2032	43.3960	43.4617	44.6007	31.4002	31.8773	31.8773	31.7563	31.7497	**31.6374**
	8	37.3436	27.8897	29.0136	29.0010	31.2571	25.7014	32.4086	33.6764	33.5048	33.6927	33.1813	**34.2064**
	16	12.2030	12.9807	15.2030	15.1420	17.4485	12.9791	37.0565	36.9978	36.3115	36.3289	35.7132	**36.9983**
3	3	0.0017	8.13e-05	8.13e-05	8.13e-05	0.0005	8.13e-05	75.8034	89.0256	89.0256	89.0256	80.3664	**89.0256**
	5	0.0012	8.13e-05	8.13e-05	8.13e-05	74.7289	8.39e-05	77.2376	89.0256	89.0256	89.0256	29.3959	**88.8920**
	8	8.13e-05	8.39e-05	8.13e-05	8.13e-05	0.0008	8.13e-05	89.0256	88.8920	89.0256	89.0256	78.8657	**89.0256**
	16	1.47e-04	8.13e-05	8.64e-05	8.64e-05	0.0009	8.13e-05	86.4428	89.0256	88.7623	88.7623	78.5870	**89.0256**
4	3	5.92e-04	1.04e-04	2.54e-06	1.52e-05	3.81e-05	1.04e-04	80.4036	87.9493	104.0771	96.2956	92.3162	**87.9493**
	5	2.54e-06	1.04e-04	2.54e-06	2.54e-06	0.0001	3.94e-04	104.0771	87.9493	104.0771	104.0771	85.9479	**82.1738**
	8	3.58 e-04	1.04e-04	1.11e-04	1.52e-05	0.0001	1.06e-05	82.5849	87.9493	87.6426	96.2956	87.2647	**97.8777**
	16	1.75 e-04	3.00e-04	1.11e-04	1.52e-05	0.0039	1.08e-04	85.6886	83.3583	87.6426	96.2956	72.1181	**87.7966**
5	3	31.9777	82.6362	84.9997	82.6362	87.6667	82.6362	33.0823	28.9591	28.8366	28.9590	28.7024	**28.9591**
	5	28.4928	49.2085	53.3347	56.8345	52.0450	53.3347	33.5835	31.2104	30.8607	30.5846	30.9670	**30.8607**
	8	39.4756	41.1431	38.5217	38.2350	44.7939	36.7723	32.2160	31.9878	32.2738	32.3061	31.6186	**32.4756**
	16	3.81 e-06	24.9071	23.6980	22.5317	27.7335	3.81e-06	102.3162	34.1676	34.3837	34.6028	33.7335	**102.3162**
6	3	11.6380	11.4073	11.4073	11.4073	12.1655	11.6036	37.4720	37.5590	37.5590	37.5589	37.2794	**37.4849**
	5	14.4554	12.9366	12.9366	12.9628	14.2037	12.9238	36.5305	37.0126	37.0126	37.0038	36.6067	**37.0169**
	8	2.9898	4.6143	4.1842	3.7919	17.7893	2.4275	43.3744	41.4897	41.9146	42.3421	35.6291	**44.2792**
	16	0.0215	4.4226	6.1143	4.1916	11.8977	4.7886	64.8157	41.6740	40.2673	41.9069	37.3761	**40.5051**
7	3	151.7378	173.3686	173.3656	173.3656	174.1420	199.9488	26.3199	25.7412	25.7412	25.7411	25.7217	**25.1216**
	5	81.9594	50.0431	58.2060	52.5064	69.6538	57.9147	28.9948	31.1374	30.4811	30.9286	29.7013	**30.5029**
	8	10.7962	39.4852	32.1569	32.1865	35.6861	30.5212	37.7981	32.1665	33.0581	33.0541	32.6058	**33.2848**
	16	0.0109	5.3824	3.9797	2.1201	0.9462	3.2652	67.7723	40.8211	42.1323	44.8671	48.3707	**42.9917**
8	3	140.8190	5.20e-05	140.8208	5.20e-05	140.8225	140.8208	26.6442	90.9708	26.6441	90.9707	26.6440	**26.6441**
	5	2.0130	5.20e-05	116.0839	5.20e-05	121.5940	107.3783	45.0923	90.9708	27.4831	90.9707	27.2816	**27.8216**
	8	0.1431	5.20e-05	5.20e-05	5.20e-05	6.2815	3.9177	56.5750	90.9708	90.9708	90.9707	40.1501	**42.2005**

Table 8 (continued)

Test images	M	MSE						PSNR					
		BAT	BSA	FA	PSO	WDO	EMO	BAT	BSA	FA	PSO	WDO	EMO
	16	4.6572	1.36e-04	7.60e-05	2.4e-04	4.0803	1.16e-04	41.4495	86.7954	89.3227	84.1862	42.0238	**87.4862**
9	3	13.1164	4.92e-04	12.3187	4.92e-04	13.0716	13.6969	36.9526	81.2103	37.2252	81.2103	36.9674	**36.7646**
	5	0.8931	4.92e-04	4.92e-04	4.92e-04	0.0930	3.3910	48.6218	81.2103	81.2103	81.2103	58.4423	**42.8276**
	8	4.92e-04	4.92e-04	4.92e-04	4.92e-04	0.2826	4.92e-04	81.2103	81.2103	81.2103	81.2103	53.6183	**81.2103**
	16	5.4551	4.92e-04	6.17e-04	5.30e-04	0.0013	6.17e-04	40.7628	81.2103	80.2211	80.8860	76.7051	**80.2211**
10	3	1.3245	1.73e-06	1.6984	1.731e-06	1.3690	1.73e-06	46.9101	105.7471	45.8304	105.7470	46.7666	**105.7471**
	5	0.6120	1.73e-06	1.73e-06	6.92e-06	4.0181	1.73e-06	50.2630	105.7471	105.7471	99.7264	42.0905	**105.7471**
	8	8.31 e-05	1.73e-06	3.46e-06	1.73e-06	3.4626	1.73e-06	88.9347	105.7471	102.7368	105.7470	102.7367	**105.7471**
	16	0.0495	1.73e-05	3.46e-06	3.46e-06	0.0018	8.65e-06	61.1857	95.7471	102.7368	102.7367	75.3967	**98.7574**

Table 9 Comparison of SSIM, and FSIM computed by different algorithm using Kapur's entropy

Test images	M	SSIM						FSIM					
		BAT	BSA	FA	PSO	WDO	EMO	BAT	BSA	FA	PSO	WDO	EMO
1	3	0.6412	0.6178	0.6178	0.6178	0.6118	0.6175	0.7905	0.7889	0.7889	0.7889	0.7878	0.7888
	5	0.6978	0.7505	0.7505	0.7486	0.7485	0.7506	0.7999	0.8776	0.8776	0.8754	0.8765	0.8784
	8	0.8307	0.8365	0.8365	0.8317	0.8262	0.8390	0.9254	0.9331	0.9331	0.9300	0.9315	0.9345
	16	0.9058	0.9289	0.9221	0.9113	0.8919	0.9294	0.9647	0.9834	0.9803	0.9700	0.9667	0.9878
2	3	0.4845	05503	0.5503	0.5502	0.5491	0.5524	0.7754	0.8065	0.8065	0.8064	0.8066	0.8077
	5	0.6265	0.6735	0.6735	0.6710	0.6721	0.6792	0.8460	0.8859	0.8859	0.8894	0.8845	0.8834
	8	0.7497	0.7727	0.7757	0.7612	0.7619	0.7631	0.9148	0.9367	0.9377	0.9299	0.9315	0.9316
	16	0.9099	0.8927	0.9001	0.8548	0.8840	0.8992	0.9702	0.9773	0.9765	0.9649	0.9746	0.9790
3	3	0.6500	0.6449	0.6449	0.6181	0.6443	0.6580	0.8395	0.8397	0.8397	0.8292	0.8391	0.7888
	5	0.6432	0.7265	0.7665	0.7866	0.7219	0.7881	0.8561	0.8893	0.8980	0.9020	0.8888	0.8754
	8	0.8437	0.8882	0.8865	0.8843	08270	0.8924	0.9246	0.9527	0.9524	0.9508	0.9274	0.9621
	16	0.9320	0.9653	0.9668	0.9524	0.9648	0.9397	0.9793	0.9931	0.9935	0.9882	0.9924	0.9978
4	3	0.3884	0.6225	0.5991	0.6224	0.6231	0.5991	0.7395	0.7593	0.7511	0.7593	0.7594	0.8397
	5	0.7713	0.7890	0.7586	0.7568	0.8038	0.7545	0.8264	0.8402	0.8259	0.8261	0.8487	0.9024
	8	0.8446	0.8512	0.8545	0.8585	0.8435	0.8590	0.8959	0.9050	0.9061	0.9157	0.8980	0.9536
	16	0.9100	0.9255	0.9342	0.9167	0.9130	0.9346	0.9444	0.9696	0.9748	0.9540	0.9572	0.9788
5	3	0.6754	0.6809	0.6809	0.6809	0.6793	0.6882	0.8320	0.8473	0.8473	0.8473	0.8485	0.7511
	5	0.7510	0.7564	0.7564	0.7590	0.7515	0.7497	0.8998	0.9030	0.9030	0.9040	0.9004	0.9188
	8	0.7652	0.8422	0.8375	0.8327	0.8260	0.8510	0.8889	0.9472	0.9447	0.9399	0.9395	0.9528
	16	0.9130	0.9239	0.9330	0.9018	0.9176	0.9213	0.9739	0.9787	0.9834	0.9656	0.9746	0.9721
6	3	0.6497	0.6119	0.6119	0.6118	0.3133	0.6174	0.7609	0.7557	0.7557	0.7557	0.6782	0.8506
	5	0.7785	0.7536	0.7581	0.7539	0.7512	0.7912	0.8947	0.8778	0.8781	0.8737	0.8539	0.9003
	8	0.7792	0.8187	0.8316	0.8226	0.8541	0.8548	0.9132	0.9445	0.9464	0.9370	0.9409	0.9471
	16	0.9031	0.8966	0.8885	0.8931	0.8975	0.8891	0.9705	0.9754	0.9752	0.9721	0.9760	0.9765
7	3	0.4389	0.2552	0.2630	0.3607	0.3514	0.3608	0.7674	0.7074	0.7101	0.7483	0.7458	0.7483
	5	0.8077	0.7497	0.7369	0.7466	0.7834	0.7288	0.8843	0.8839	0.8820	0.8825	0.8923	0.8779
	8	0.9045	0.8269	0.8867	0.8464	0.8936	0.9052	0.9859	0.9174	0.9334	0.9224	0.9362	0.9439
	16	0.9687	0.9654	0.9740	0.9376	0.9638	0.9744	0.9891	0.9843	0.9912	0.9620	0.9841	0.9926
8	3	0.3161	0.3916	0.3916	0.3915	0.3875	0.3980	0.7679	0.8171	0.8171	0.8171	0.8161	0.7578
	5	0.7515	0.5162	0.5162	0.5162	0.5020	0.5246	0.8962	0.8767	0.8767	0.8767	0.8765	0.9014
	8	0.8878	0.6287	0.8584	0.6821	0.6166	0.6242	0.9365	0.9079	0.9667	0.9144	0.9070	0.9373

Table 9 (continued)

Test images	M	SSIM						FSIM					
		BAT	BSA	FA	PSO	WDO	EMO	BAT	BSA	FA	PSO	WDO	EMO
	16	0.9316	0.9575	0.9547	0.9080	0.9331	0.9594	0.9831	0.9952	0.9945	0.9868	0.9896	0.9930
9	3	0.6425	0.6702	0.6118	0.6701	0.6165	0.6024	0.7847	0.7843	0.7840	0.7842	0.7832	0.7719
	5	0.7461	0.7689	0.7701	0.7687	0.7749	0.7697	0.8556	0.8796	0.8828	0.8798	0.8854	0.8869
	8	0.8600	0.8712	0.8651	0.8589	0.8651	0.8740	0.9339	0.9431	0.9415	0.9376	0.9401	0.9436
	16	0.9068	0.9408	0.9394	0.9354	0.9347	0.9410	0.9617	0.9852	0.9837	0.9772	0.9783	0.9834
10	3	0.5698	0.5701	0.5701	0.5701	0.5654	0.5701	0.7896	0.7828	0.7828	0.7828	0.7831	0.8171
	5	0.7546	0.7641	0.7716	0.7586	0.7735	0.7625	0.9105	0.9210	0.9218	0.9211	0.9167	0.8778
	8	0.7914	0.8588	0.8560	0.8561	0.8527	0.8627	0.9251	0.9578	0.9559	0.9527	0.9510	0.9630
	16	0.9303	0.9510	0.9492	0.9435	0.9419	0.9566	0.9872	0.9878	0.9939	0.9865	0.9831	0.9941

Table 10 Comparison of SSIM, and FSIM computed by different algorithm using Tsallis entropy

Test images	M	SSIM						FSIM					
		BAT	BSA	FA	PSO	WDO	EMO	BAT	BSA	FA	PSO	WDO	EMO
1	3	0.6196	0.6254	0.6414	0.6253	0.6362	0.6254	0.7580	0.7599	0.7531	0.7590	0.7775	0.7799
	5	0.7623	0.7538	0.7463	0.7534	0.7628	0.7249	0.8751	0.8609	0.8546	0.8614	0.8745	0.8368
	8	0.8172	0.8384	0.8332	0.8371	0.8459	0.8461	0.9104	0.9290	0.9225	0.9277	0.9370	0.9376
	16	0.8297	0.9321	0.9346	0.9111	0.9039	0.9434	0.8989	0.9748	0.9850	0.9663	0.9621	0.9792
2	3	0.5398	0.5503	0.5503	0.5502	0.5469	0.5510	0.7896	0.8065	0.8605	0.8064	0.8055	0.8067
	5	0.7003	0.6735	0.6735	0.6737	0.6658	0.6735	0.8811	0.8859	0.8859	0.8859	0.8829	0.8865
	8	0.7496	0.7723	0.7784	0.7818	0.7673	0.7818	0.9209	0.9369	0.9389	0.9370	0.9343	0.9466
	16	0.8975	0.8926	0.9009	0.8714	0.9145	0.9287	0.9708	0.9770	0.9793	0.9684	0.9808	0.9860
3	3	0.5560	0.5619	0.5372	0.5615	0.5894	0.5615	0.7110	0.7409	0.7532	0.7388	0.7592	0.7388
	5	0.7770	0.8084	0.7993	0.8078	0.8088	0.8094	0.8411	0.9179	0.9095	0.9152	0.9196	0.9199
	8	0.8842	0.9022	0.8950	0.8968	0.8783	0.8949	0.9598	0.9728	0.9544	0.9712	0.9513	0.9728
	16	0.9569	0.9671	0.9642	0.9521	0.9574	0.9697	0.9882	0.9945	0.9931	0.9912	0.9908	0.9940
4	3	0.6988	0.7234	0.7239	0.7234	0.7088	0.7235	0.7496	0.7633	0.7629	0.7633	0.7505	0.7628
	5	0.7585	0.7840	0.8069	0.7234	0.8237	0.7838	0.8033	0.8330	0.8483	0.7633	0.8552	0.8343
	8	0.8499	0.8656	0.8657	0.8691	0.8621	0.8790	0.8906	0.9139	0.9140	0.9161	0.9120	0.9167
	16	0.9201	0.9356	0.9254	0.9242	0.9347	0.9319	0.9421	0.9758	0.9690	0.9594	0.9734	0.9774
5	3	0.6742	0.6841	0.6841	0.6841	0.6841	0.6729	0.8391	0.8476	0.8476	0.8475	0.8475	0.8449
	5	0.7459	0.7564	0.7564	0.7545	0.7528	0.7642	0.8836	0.9030	0.9030	0.9021	0.9018	0.9044
	8	0.8009	0.8410	0.8441	0.8502	0.8373	0.8681	0.9262	0.9472	0.9471	0.9476	0.9437	0.9520
	16	0.8818	0.9239	0.9231	0.9070	0.9169	0.9166	0.9576	0.9787	0.9797	0.9708	0.9749	0.9794
6	3	0.6054	0.6161	0.6161	0.6161	0.6958	0.6161	0.7689	0.7582	0.7582	0.7582	0.8194	0.7582
	5	0.7964	0.7536	0.7892	0.7534	0.7428	0.7974	0.9046	0.8778	0.8956	0.8773	0.8741	0.8993
	8	0.7991	0.8187	0.8301	0.8560	0.8418	0.8562	0.9411	0.9445	0.9406	0.9394	0.9444	0.9459
	16	0.8863	0.8984	0.8950	0.8885	0.9222	0.9166	0.9680	0.9755	0.9773	0.9681	0.9692	0.9853
7	3	0.4053	0.2552	0.3308	0.3607	0.3061	0.3061	0.7387	0.7074	0.7351	0.7483	0.7305	0.7302
	5	0.6798	0.7497	0.7307	0.7271	0.7427	0.7497	0.8563	0.8839	0.8783	0.8790	0.8807	0.8839
	8	0.8351	0.8243	0.8239	0.8611	0.8155	0.8201	0.9107	0.9168	0.9165	0.9270	0.9139	0.9317
	16	0.9736	0.9681	0.9760	0.9623	0.9529	0.9775	0.9913	0.9871	0.9943	0.9824	0.9737	0.9950
8	3	0.3991	0.5964	0.3991	0.5991	0.3930	0.5964	0.8125	0.8212	0.8187	0.8217	0.8190	0.8221
	5	0.5499	0.7736	0.5162	0.7722	0.4944	0.7670	0.8727	0.9407	0.8767	0.9394	0.8757	0.9303
	8	0.8710	0.8682	0.8206	0.8634	0.8663	0.8728	0.9485	0.9746	0.9633	0.9722	0.9690	0.9755

Table 10 (continued)

Test images	M	SSIM						FSIM					
		BAT	BSA	FA	PSO	WDO	EMO	BAT	BSA	FA	PSO	WDO	EMO
	16	0.9569	0.9566	0.9493	0.9546	0.9279	0.9547	0.9941	0.9943	0.9938	0.9932	0.9868	0.9953
9	3	0.6770	0.6706	0.6695	0.6705	0.6596	0.6582	0.7452	0.7455	0.7754	0.7454	0.7616	0.7804
	5	0.7363	0.7664	0.7870	0.7663	0.8087	0.7664	0.8244	0.8695	0.8783	0.8694	0.8933	0.8695
	8	0.8656	0.8650	0.8370	0.8644	0.8626	0.8674	0.9290	0.9417	0.9195	0.9402	0.9392	0.9440
	16	0.9063	0.9361	0.9376	0.9291	0.9271	0.9337	0.9558	0.9833	0.9833	0.9745	0.9742	0.9800
10	3	0.6475	0.5359	0.6414	0.5359	0.5687	0.5344	0.8397	0.7763	0.8439	0.7763	0.7821	0.7763
	5	0.7995	0.7374	0.7038	0.7373	0.7782	0.7181	0.9399	0.9154	0.8896	0.9153	0.9259	0.9287
	8	0.8420	0.8470	0.8512	0.8332	0.8546	0.8449	0.9576	0.9589	0.9625	0.9520	0.9533	0.9773
	16	0.9276	0.9529	0.9555	0.9383	0.9064	0.9562	0.9872	0.9529	0.9956	0.9893	0.9722	0.9870

Table 11 Comparison SSIM, and FSIM computed by different algorithm using Renyi entropy

Test images	M	SSIM						FSIM					
		BAT	BSA	FA	PSO	WDO	EMO	BAT	BSA	FA	PSO	WDO	EMO
1	3	0.6561	0.6254	0.6265	0.6254	0.6364	0.6369	0.7665	0.7599	0.7575	0.7599	0.7785	**0.7769**
	5	0.7514	0.7538	0.7517	0.7365	0.7654	0.7643	0.8660	0.8615	0.8576	0.8477	0.8777	**0.8777**
	8	0.7515	0.8390	0.8374	0.8393	0.8301	0.8397	0.8469	0.9297	0.9272	0.9303	0.9197	**0.9389**
	16	0.8961	0.9323	0.9325	0.9100	0.9206	0.9341	0.9577	0.9849	0.9846	0.9648	0.9715	**0.9850**
2	3	0.5335	0.5503	0.5503	0.5502	0.5492	0.5600	0.7980	0.8065	0.8065	0.8064	0.8063	**0.8104**
	5	0.6588	0.6735	0.6735	0.6711	0.6724	0.6671	0.8762	0.8859	0.8859	0.8851	0.8860	**0.8826**
	8	0.7216	0.7755	0.7727	0.7742	0.7685	0.7799	0.9048	0.9376	0.9367	0.9376	0.9343	**0.9385**
	16	0.9172	0.8922	0.8779	0.8502	0.8771	0.8873	0.9756	0.9760	0.9729	0.9655	0.9732	**0.9769**
3	3	0.5900	0.5922	0.5577	0.5922	0.5985	0.6056	0.7415	0.7646	0.7690	0.7646	0.7707	**0.7753**
	5	0.7037	0.8084	0.7996	0.8084	0.7327	0.8183	0.8193	0.9179	0.9053	0.9178	0.8897	**0.9256**
	8	0.8086	0.9022	0.9071	0.9005	0.8925	0.9102	0.8946	0.9728	0.9571	0.9695	0.9614	**0.9755**
	16	0.9570	0.9661	0.9695	0.9572	0.9613	0.9563	0.9849	0.9950	0.9943	0.9904	0.9894	**0.9924**
4	3	0.6775	0.7209	0.7209	0.7208	0.7213	0.7213	0.7341	0.7587	0.7586	0.7586	0.7595	**0.7580**
	5	0.7888	0.8228	0.8228	0.8109	0.8097	0.7853	0.8288	0.8575	0.8574	0.8488	0.8452	**0.8351**
	8	0.8630	0.8672	0.8662	0.8706	0.8723	0.8739	0.9041	0.9151	0.9149	0.9160	0.9178	**0.9180**
	16	0.9138	0.9397	0.9345	0.9157	0.9418	0.9418	0.9441	0.9790	0.9747	0.9550	0.9768	**0.9795**
5	3	0.7104	0.6841	0.6778	0.6841	0.6834	0.6841	0.8551	0.8476	0.8448	0.8475	0.8451	**0.8476**
	5	0.7419	0.7577	0.7553	0.7550	0.7557	0.7553	0.8882	0.9043	0.9033	0.9025	0.9022	**0.9039**
	8	0.8425	0.8427	0.8451	0.8380	0.8345	0.8515	0.9413	0.9471	0.9478	0.9430	0.9369	**0.9482**
	16	0.9039	0.9230	0.9227	0.9137	0.9104	0.9243	0.9704	0.9780	0.9782	0.9793	0.9713	**0.9782**
6	3	0.6298	0.6213	0.6213	0.6212	0.6300	0.6308	0.7658	0.7598	0.7598	0.7598	0.7597	**0.7826**
	5	0.7589	0.7536	0.7536	0.7339	0.7490	0.7505	0.8820	0.8778	0.8778	0.8728	0.9006	**0.8808**
	8	0.8007	0.8353	0.8322	0.8244	0.8244	0.8366	0.9306	0.9474	0.9460	0.9402	0.9394	**0.9474**
	16	0.8756	0.8966	0.8978	0.8756	0.8991	0.9073	0.9651	0.9754	0.9774	0.9637	0.9761	**0.9860**
7	3	0.4419	0.3791	0.3791	0.3791	0.3801	0.2871	0.7733	0.7536	0.7536	0.7535	0.7544	**0.7172**
	5	0.7101	0.7497	0.7196	0.7313	0.7222	0.7101	0.8752	0.8839	0.8752	0.8788	0.8770	**0.8700**
	8	0.9312	0.8322	0.8691	0.8730	0.8747	0.8810	0.9640	0.9183	0.9260	0.9263	0.9288	**0.9296**
	16	0.9636	0.9704	0.9695	0.9667	0.9771	0.9820	0.9902	0.9873	0.9890	0.9904	0.9940	**0.9882**
8	3	0.3879	0.5875	0.3876	0.5875	0.3880	0.3876	0.8146	0.8158	0.8162	0.8158	0.8165	**0.8162**
	5	0.7832	0.7736	0.5162	0.7724	0.5433	0.5439	0.9124	0.9407	0.8767	0.9403	0.8767	**0.8815**
	8	0.8159	0.8500	0.8273	0.8170	0.8499	0.8592	0.9594	0.9470	0.9403	0.9501	0.9652	**0.9678**

Table 11 (continued)

Test images	M	SSIM						FSIM					
		BAT	BSA	FA	PSO	WDO	EMO	BAT	BSA	FA	PSO	WDO	EMO
	16	0.9352	0.9599	0.9362	0.9512	0.9346	0.9605	0.9860	0.9927	0.9921	0.9912	0.9854	**0.9935**
9	3	0.6567	0.6701	0.6726	0.6701	0.6712	0.6662	0.7862	0.7481	0.7828	0.7480	0.7807	**0.7755**
	5	0.7677	0.7662	0.7820	0.7662	0.7934	0.7903	0.8651	0.8689	0.8732	0.8688	0.8903	**0.8861**
	8	0.8193	0.8650	0.7692	0.8623	0.8745	0.8747	0.8946	0.9417	0.8096	0.9398	0.9425	**0.9425**
	16	0.9141	0.9372	0.9269	0.9235	0.9244	0.9250	0.9650	0.9833	0.9779	0.9708	0.9740	**0.9849**
10	3	0.6235	0.5359	0.5703	0.5359	0.5129	0.5129	0.8258	0.7763	0.7845	0.7763	0.7835	**0.7612**
	5	0.7354	0.7374	0.7314	0.7338	0.7334	0.7374	0.9120	0.9154	0.9032	0.9147	0.9254	**0.9254**
	8	0.7652	0.8503	0.8292	0.8606	0.8338	0.8639	0.9156	0.9591	0.9481	0.9665	0.9588	**0.9665**
	16	0.9304	0.9455	0.9455	0.9401	0.9455	0.9510	0.9870	0.9860	0.9929	0.9907	0.9879	**0.9936**

Table 12 Comparison of CPU Timing obtained by using different methods for each sample images

Test images	*M*	Kapur's						Tsallis		
		BAT	BSA	FA	PSO	WDO	EMO	BAT	BSA	FA
1	3	8.1109	9.1994	3.7463	7.6826	5.6297	3.4930	8.5968	9.8337	3.9108
	5	9.2044	10.4636	4.3898	8.6850	6.1939	4.1780	10.1209	10.5929	4.4927
	8	10.3306	11.7188	5.5799	10.5080	7.5695	5.3985	10.9565	12.2195	5.5915
	16	14.2829	15.7633	8.5793	15.0416	10.5395	8.3964	15.39552	16.0232	8.6107
2	3	17.7382	20.8751	5.2269	16.1667	10.7878	4.6744	38.6765	22.0723	5.5985
	5	18.6371	21.9887	5.1313	17.6396	11.0633	4.4812	19.1850	22.5089	5.2336
	8	19.6271	23.0219	4.8840	19.9736	11.5706	4.2649	20.8946	24.0899	4.8634
	16	22.1830	27.4347	4.9882	25.0345	12.3730	4.5629	23.6482	28.6471	4.9617
3	3	7.8301	8.5579	3.1546	6.8826	4.7996	2.9054	7.9402	9.1085	3.1568
	5	8.4793	9.4416	3.7036	8.0525	5.5039	3.5463	8.9288	10.0886	3.7653
	8	9.5162	10.8280	4.6447	9.3678	6.4850	4.3632	10.2118	11.2576	4.5418
	16	12.4098	14.0749	7.1367	13.3601	9.2541	6.5131	13.6561	14.8839	6.8002
4	3	7.7339	8.7871	3.1311	7.1317	4.8926	2.8965	8.3194	9.3526	3.5859
	5	8.1944	9.4721	3.7585	7.8916	5.6738	3.4945	9.1771	10.6028	4.1347
	8	10.1113	10.9050	4.5791	9.2639	6.6651	4.2597	10.4567	11.7474	4.9923
	16	12.3327	14.0823	6.9770	13.2854	9.4209	6.5761	13.9490	15.3060	7.5082
5	3	7.1925	8.1155	2.5518	6.1368	4.3305	2.3145	7.3116	8.5774	2.6049
	5	7.5869	8.7634	2.9681	7.2142	5.0086	2.7418	7.8826	9.1236	3.0299
	8	8.9278	10.2165 12.5555	3.6271	8.7146	5.5416	3.3942	8.8959	10.3720	3.7054
	16	11.3272		5.4272	11.4329	7.6494	5.1033	11.3780	13.0339	5.5044
6	3	6.8300	8.3016	2.5463	6.4302	4.2592	2.2963	7.3388	8.5044	2.6763
	5	7.7923	8.7530	2.8487	7.2125	4.7608	2.6412	7.7235	9.1496	2.9042
	8	8.4046	9.5623	3.5571	8.2518	5.2733	3.1313	8.6946	10.2350	3.4930
	16	10.6605	12.1676	4.8611	11.4663	7.2079	4.6143	11.2185	12.7636	4.9600
7	3	16.4748	18.8638	3.6484	14.5455	8.7525	2.8037	17.2038	20.8154	3.5558
	5	17.0957	19.6323	3.5549	16.0427	9.3649	2.8963	17.7358	21.1905	3.6617
	8	17.6633	21.5844	3.7341	18.3288	9.9977	2.9319	19.5631	23.1760	3.9140
	16	21.1233	25.9228	3.9897	23.3103	11.4971	3.0565	22.5994	27.3939	3.9662
8	3	6.7009	7.8651	2.3906	6.1648	4.0929	2.1484	7.2803	8.8155	2.4560
	5	7.7541	8.7240	2.7831	7.1757	4.5901	2.5151	7.7917	9.5992	2.8120
	8	8.1028	9.2739	3.4978	8.1827	5.2685	2.9939	8.9421	10.2887	3.4419

Table 12 (continued)

Test images	M	Kapur's						Tsallis		
		BAT	BSA	FA	PSO	WDO	EMO	BAT	BSA	FA
	16	10.7317	12.3785	4.7591	11.0888	6.9285	4.5146	11.1505	12.7718	4.7618
9	3	16.0814	19.0034	3.4782	14.4051	8.8618	2.7801	17.1184	20.9166	3.4762
	5	17.3068	21.8790	3.4940	16.2193	9.1609	2.8747	18.1496	21.8365	3.4526
	8	18.0030	21.6721	3.6274	18.2663	9.6078	2.9439	19.2143	23.2569	3.5197
	16	21.5402	26.0868	3.8926	23.5050	11.4654	3.0429	22.0324	28.1223	3.8893
10	3	8.3122	9.4650	3.8274	7.3705	5.6002	3.6037	8.4007	9.8703	3.8213
	5	9.7020	10.4302	4.6496	8.9160	6.5829	4.3912	9.4079	10.9825	4.7350
	8	11.0796	12.5889	6.1213	11.2264	8.1621	5.9491	11.1834	13.2624	6.3195
	16	15.4773	16.7914	10.1896	16.0347	11.8911	9.6044	15.8895	17.6462	10.1517

Test images	Tsallis			Renyi					
	PSO	WDO	EMO	BAT	BSA	FA	PSO	WDO	EMO
1	7.9707	6.0128	3.6579	8.5525	10.2919	3.8744	7.9778	6.0541	**3.5781**
	9.2522	6.6434	4.3827	9.7608	11.6720	4.5553	9.1429	6.0939	**4.2168**
	10.9735	8.0221	5.4653	11.5255	12.7141	5.6852	10.8180	7.9233	**5.4607**
	14.9923	11.1614	8.4039	15.1000	17.0034	8.7330	15.2512	11.2639	**8.3556**
2	16.5852	10.6155	4.5588	18.2013	22.3194	5.1202	16.6859	10.5816	**4.4451**
	18.2832	11.1782	4.6222	19.8482	23.7217	5.0861	18.1137	11.0288	**4.3831**
	20.1425	11.3195	4.2541	21.1575	24.0023	5.0026	20.2708	11.4787	**4.2018**
	25.7544	12.7120	4.7984	23.4583	29.5420	5.0223	25.0347	12.6094	**4.5327**
3	7.2190	5.2252	2.8618	7.9819	9.4925	3.1350	7.4463	5.4005	**2.8633**
	8.2591	5.9264	3.4273	8.6276	10.1825	3.6503	8.5041	6.0278	**3.4446**
	9.8748	6.8409	4.2375	9.6867	11.5876	4.5796	9.5626	7.0620	**4.2335**
	13.7383	9.6688	6.7015	13.2512	14.9667	6.9750	13.1183	9.6126	**6.3401**
4	7.6268	5.4566	3.2154	8.0910	9.7245	3.3803	7.6841	5.5387	**3.1483**
	7.6268	6.1689	3.9221	8.9931	10.3677	4.0522	8.8440	6.3376	**3.8891**
	10.8362	7.3508	4.7384	10.0971	11.9025	4.9518	10.4584	7.6119	**4.2264**
	14.1166	10.4125	7.3623	13.4754	14.3751	7.5849	14.3603	10.4369	**6.5718**

Table 12 (continued)

Test images	Tsallis			Renyi					
	PSO	WDO	EMO	BAT	BSA	FA	PSO	WDO	EMO
5	6.5910	4.7221	2.3553	7.2005	8.9297	2.5819	6.5548	4.5201	**2.3687**
	7.4844	5.2816	2.8231	7.6991	9.6516	3.0381	7.5841	5.1192	**2.7824**
	8.6063	6.0854	3.3410	8.7077	10.6558	3.6536	8.9611	5.9298	**3.3308**
	11.7341	8.0903	4.8929	11.1780	13.3665	5.3905	12.1623	8.0180	**4.8922**
6	6.6268	4.5885	2.2980	7.1547	8.8029	2.5762	7.0173	4.7767	**2.3090**
	7.2697	5.0179	2.6423	7.7440	9.2199	2.9036	7.8483	5.1521	**2.6419**
	8.4126	5.7351	3.1454	8.5919	10.1206	3.4479	8.2835	5.8856	**3.1284**
	11.4375	7.6096	4.5964	11.2129	12.7840	4.8710	11.2564	7.4227	**4.6093**
7	14.7921	9.0402	2.8774	16.6200	19.8152	3.5255	14.8037	9.2475	**2.8625**
	16.4060	9.5530	2.9285	18.1106	21.9094	3.6043	16.6313	9.7436	**2.8983**
	18.8213	9.8875	2.9868	18.5898	22.9628	3.6950	18.9442	10.2078	**2.9253**
	23.7157	11.4093	3.0931	22.9064	27.6976	4.0570	24.1412	11.7824	**3.0495**
8	6.6870	4.5764	2.3095	7.2711	9.0127	2.4414	6.9074	4.7123	**2.1937**
	7.4788	5.2298	2.6317	7.9724	9.9309	2.7856	7.5330	5.0659	**2.5338**
	8.4939	5.9178	3.1711	8.7725	10.8110	3.4058	8.7627	5.6357	**3.1230**
	11.4675	8.0211	4.5268	10.988	13.2370	4.8631	11.8328	7.4317	**4.5048**
9	15.1391	9.1024	2.8494	16.6167	20.3274	3.5342	14.9411	8.9903	**2.8359**
	16.5823	9.5362	2.7527	17.7547	21.7643	3.4907	16.6153	9.6230	**2.8329**
	18.8894	10.1309	2.8267	18.6780	23.2753	3.5740	19.0085	10.1322	**2.8106**
	23.7438	11.3365	2.9829	22.3292	27.1957	3.8076	23.4255	11.4317	**2.9722**
10	7.9700	5.9552	3.7198	8.3975	10.4943	3.8360	8.1758	5.7273	**3.6867**
	9.3050	6.886	4.6231	9.7151	11.6228	4.7140	9.7524	6.7172	**4.4743**
	11.3994	8.3924	6.1777	11.7045	13.6791	6.0805	11.9028	8.4489	**5.1343**
	16.4246	12.4808	9.8301	16.7586	18.2346	9.8805	17.4492	12.4615	**9.1950**

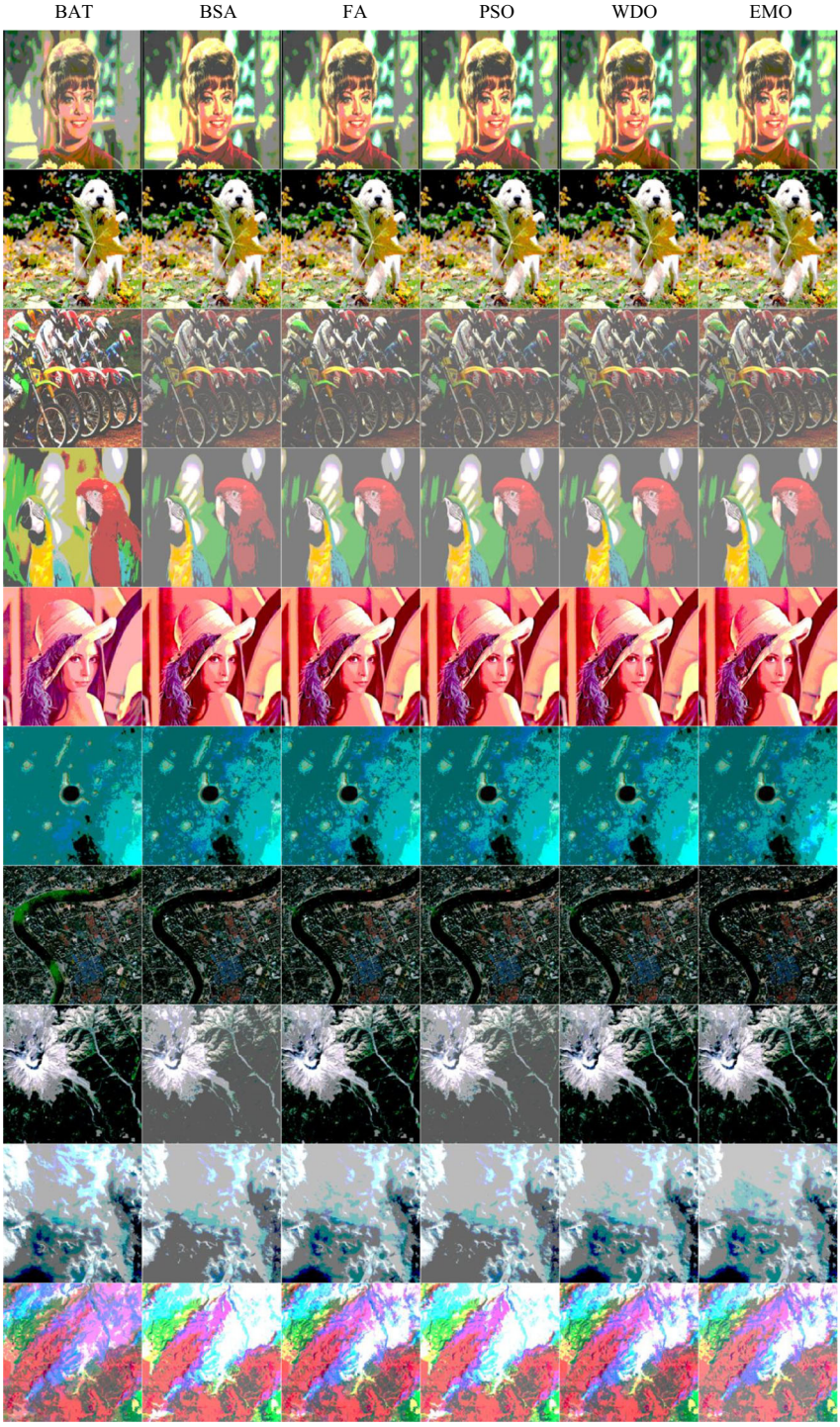

Fig. 4 The 3-levels thresholded test images obtained by BAT, BSA, FA, PSO, WDO and EMO techniques using Kapur's entropy

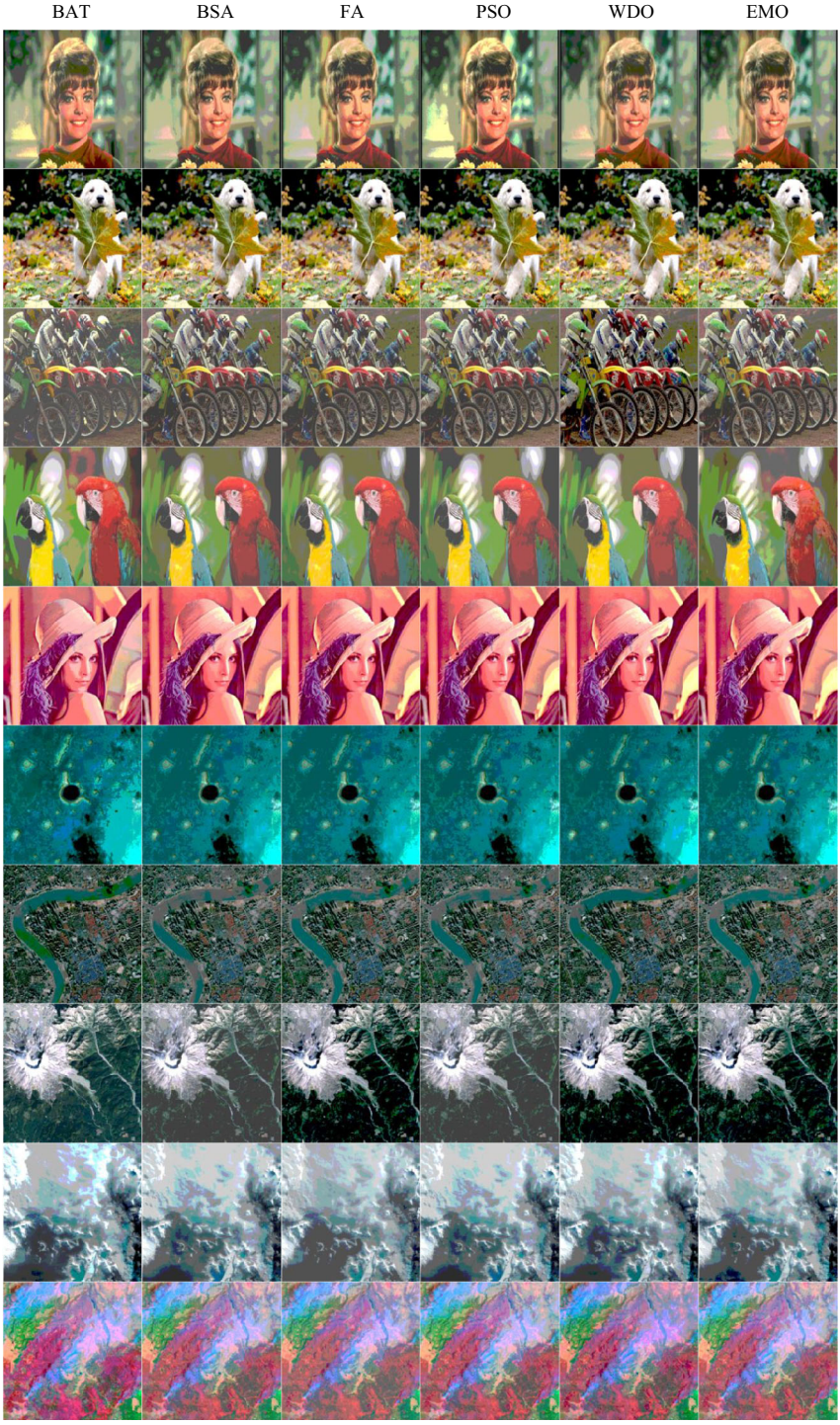

Fig. 5 The 5-levels thresholded test images obtained by BAT, BSA, FA, PSO, WDO and EMO techniques using Kapur's entropy

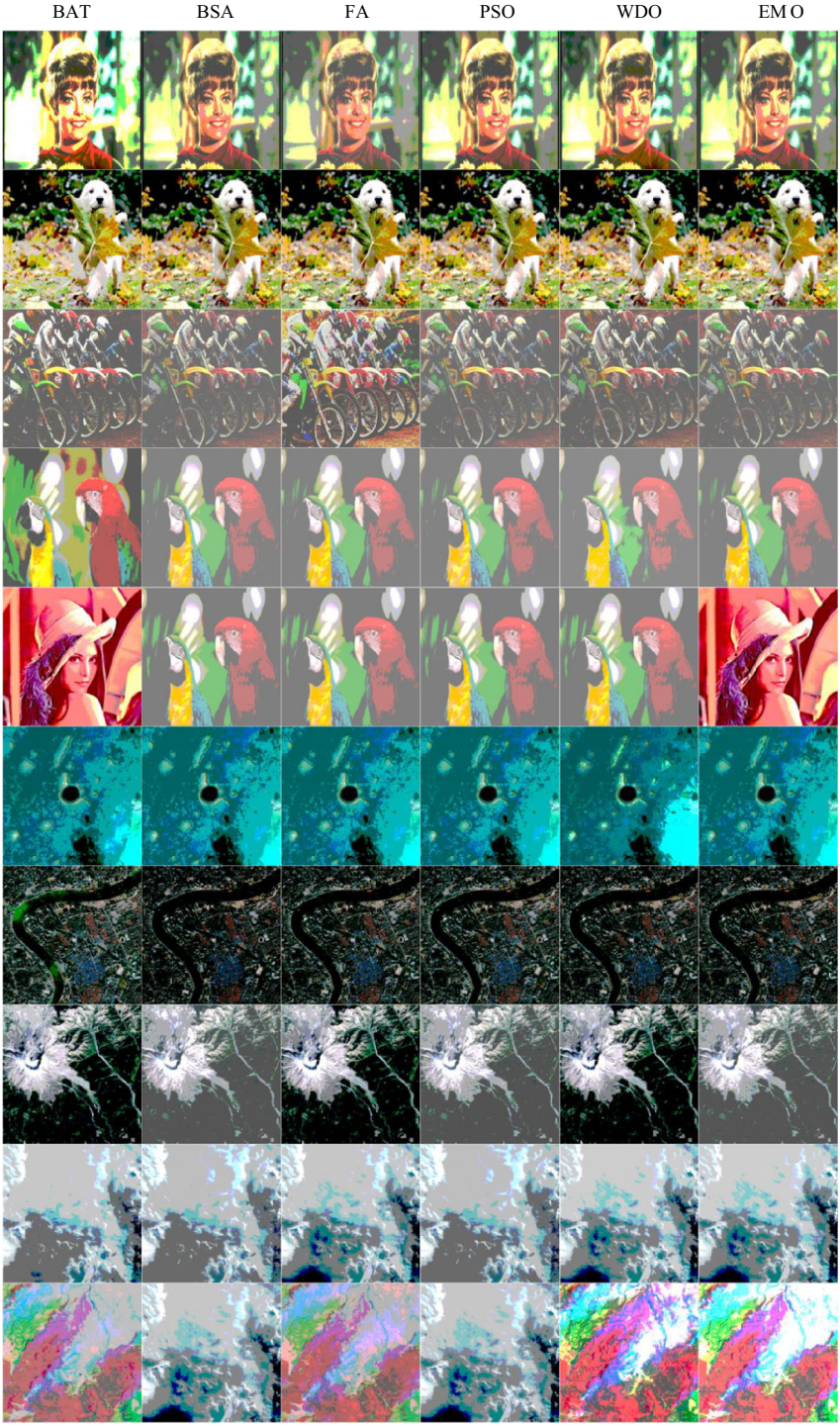

Fig. 6 The 3-levels thresholded test images obtained by BAT, BSA, FA, PSO, WDO and EMO techniques using Tsallis entropy

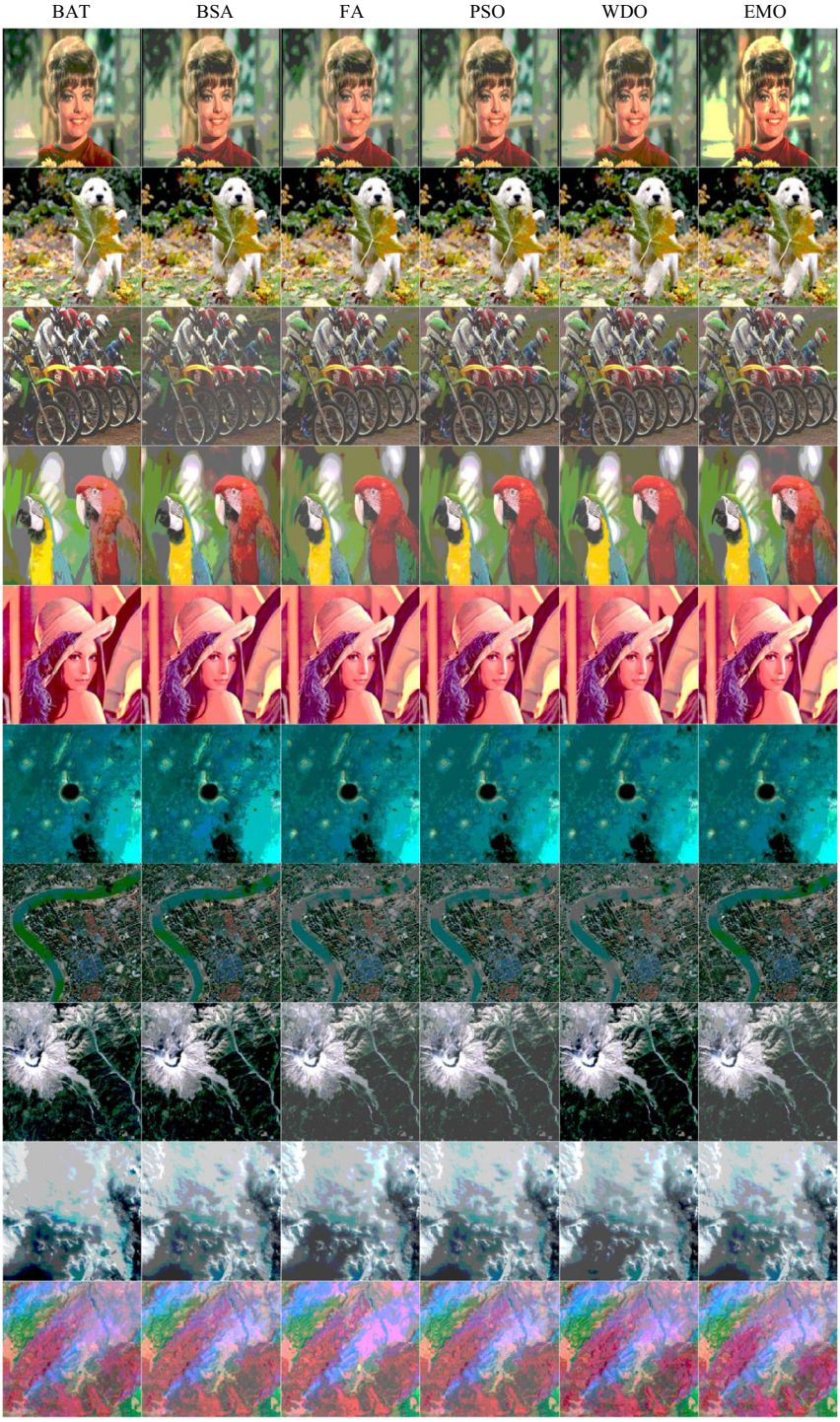

Fig. 7 The 5-levels thresholded test images obtained by BAT, BSA, FA, PSO, WDO and EMO techniques using Tsallis entropy

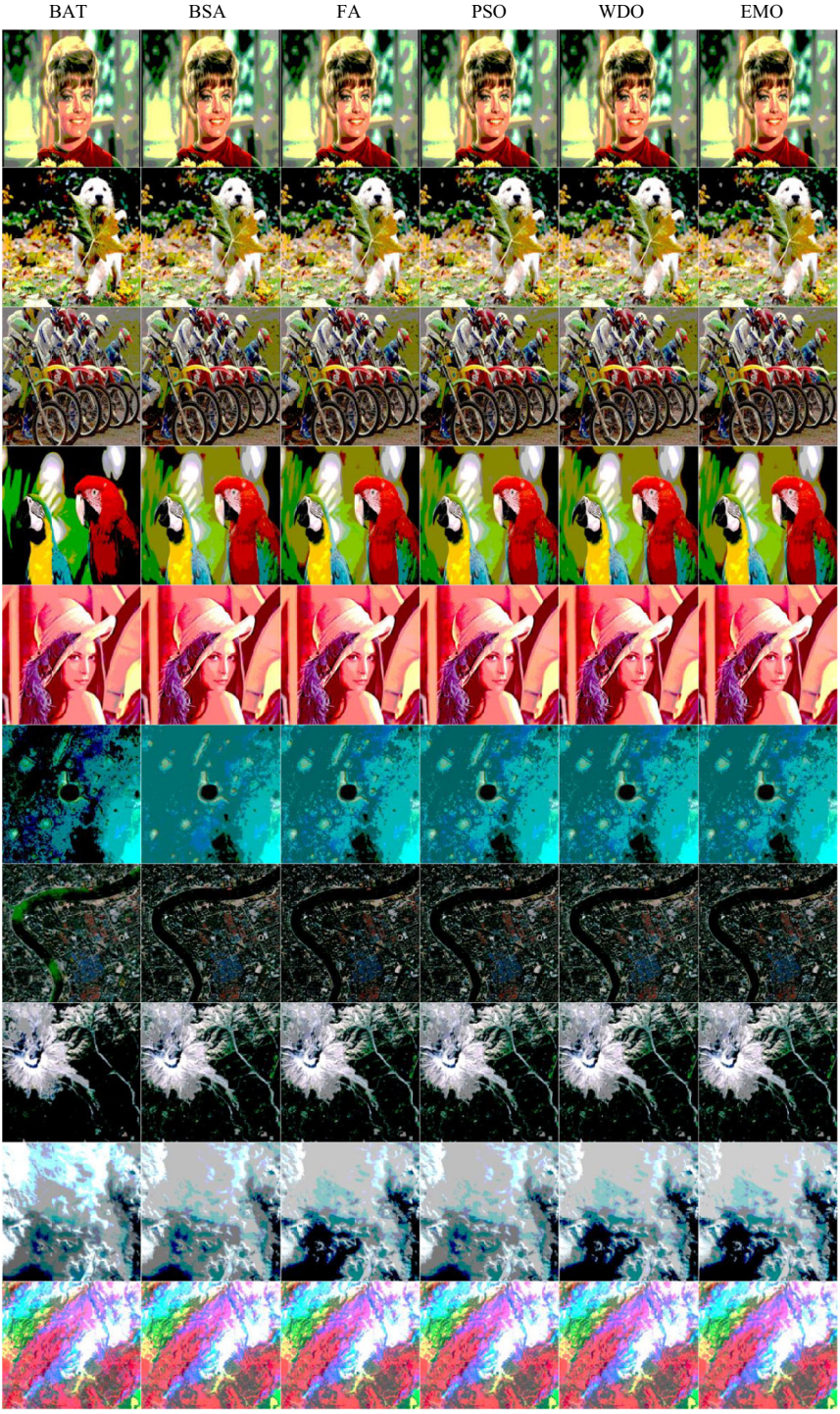

Fig. 8 The 3-levels thresholded test images obtained by BAT, BSA, FA, PSO, WDO, and EMO techniques using Renyi's entropy

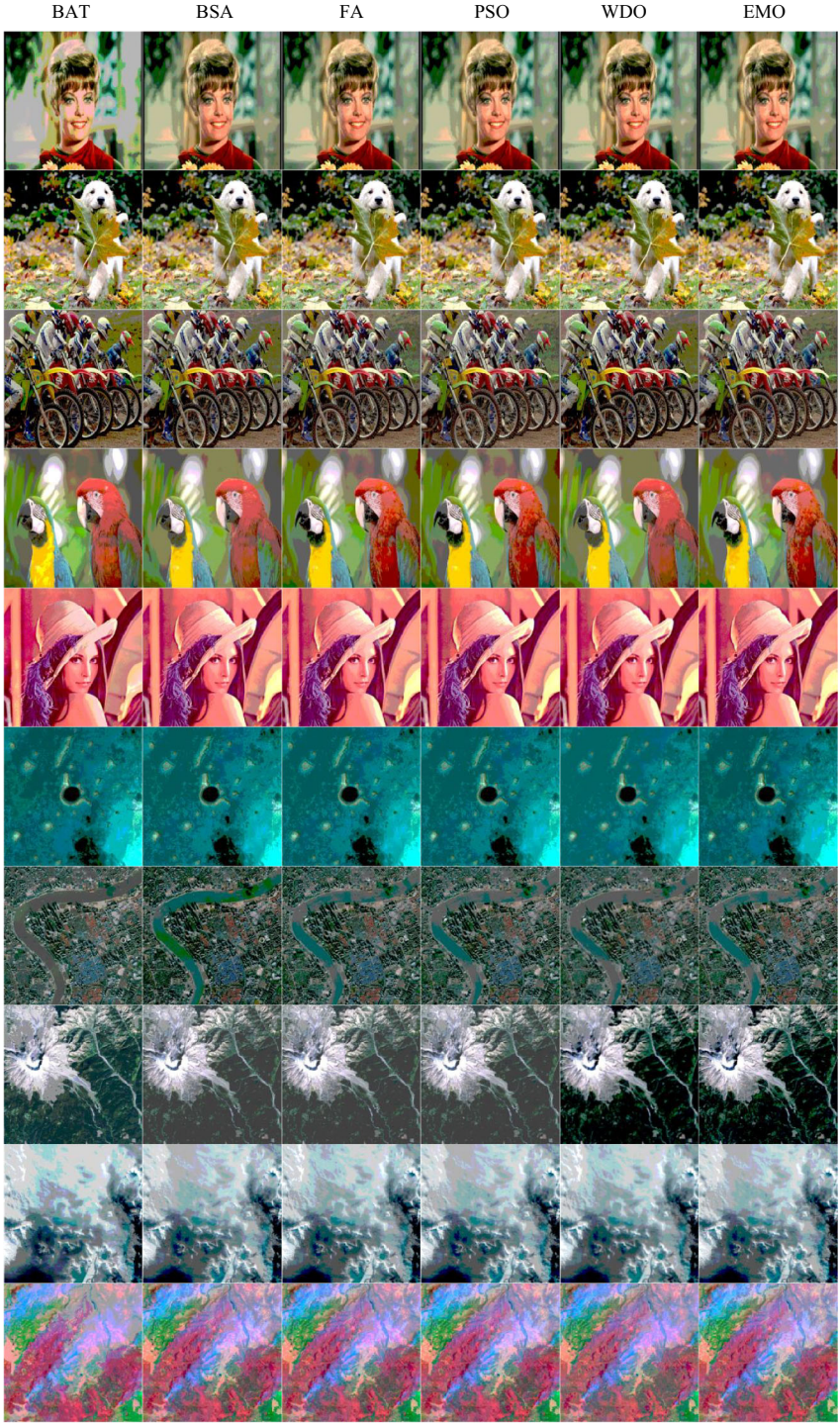

Fig. 9 The 5-levels thresholded test images obtained by BAT, BSA, FA, PSO, WDO, and EMO techniques using Renyi's entropy

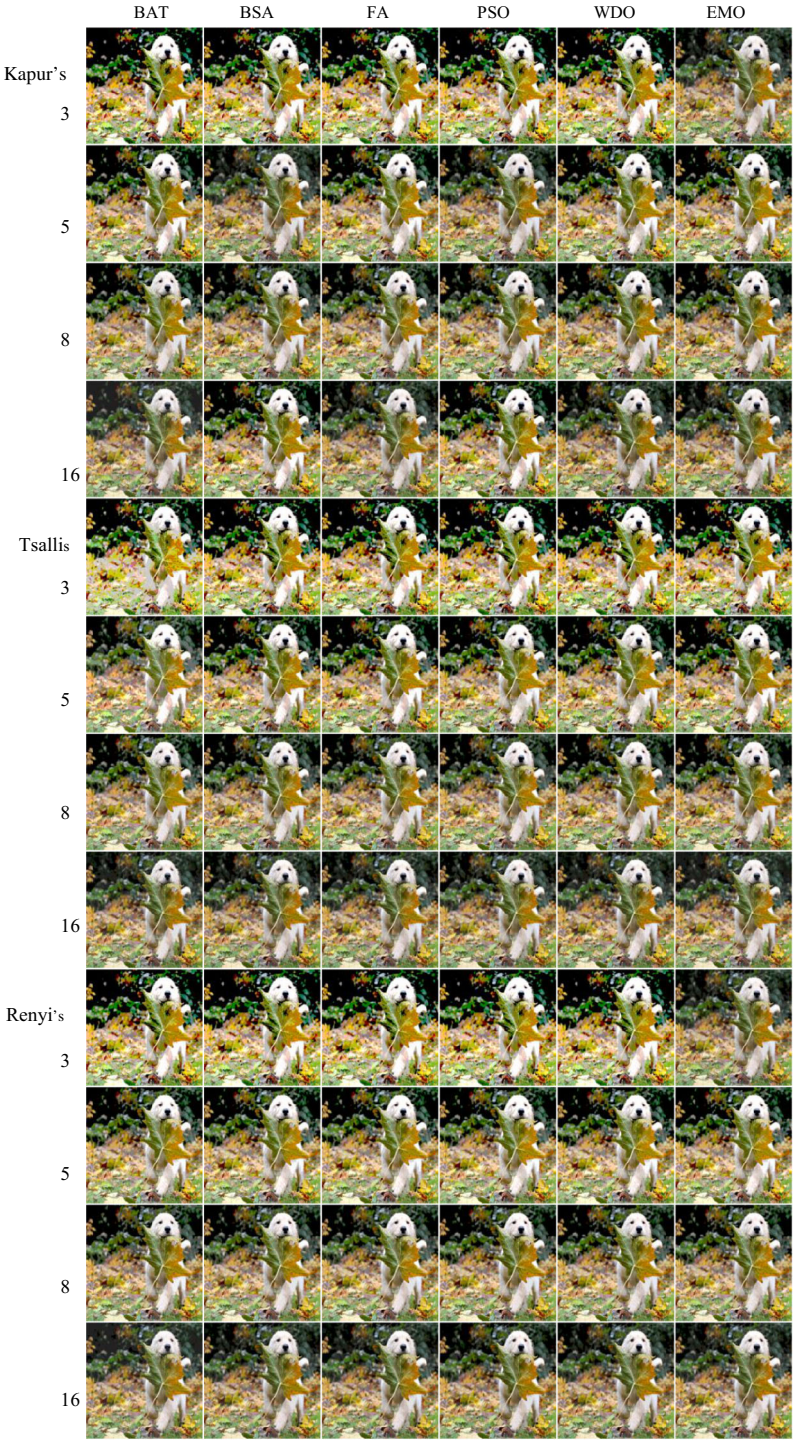

Fig. 10 The 3, 5, 8, and 16-levels thresholded test image 2 obtained by BAT, BSA, FA, PSO, WDO, and EMO techniques using Kapur's, Tsallis and Renyi's entropy

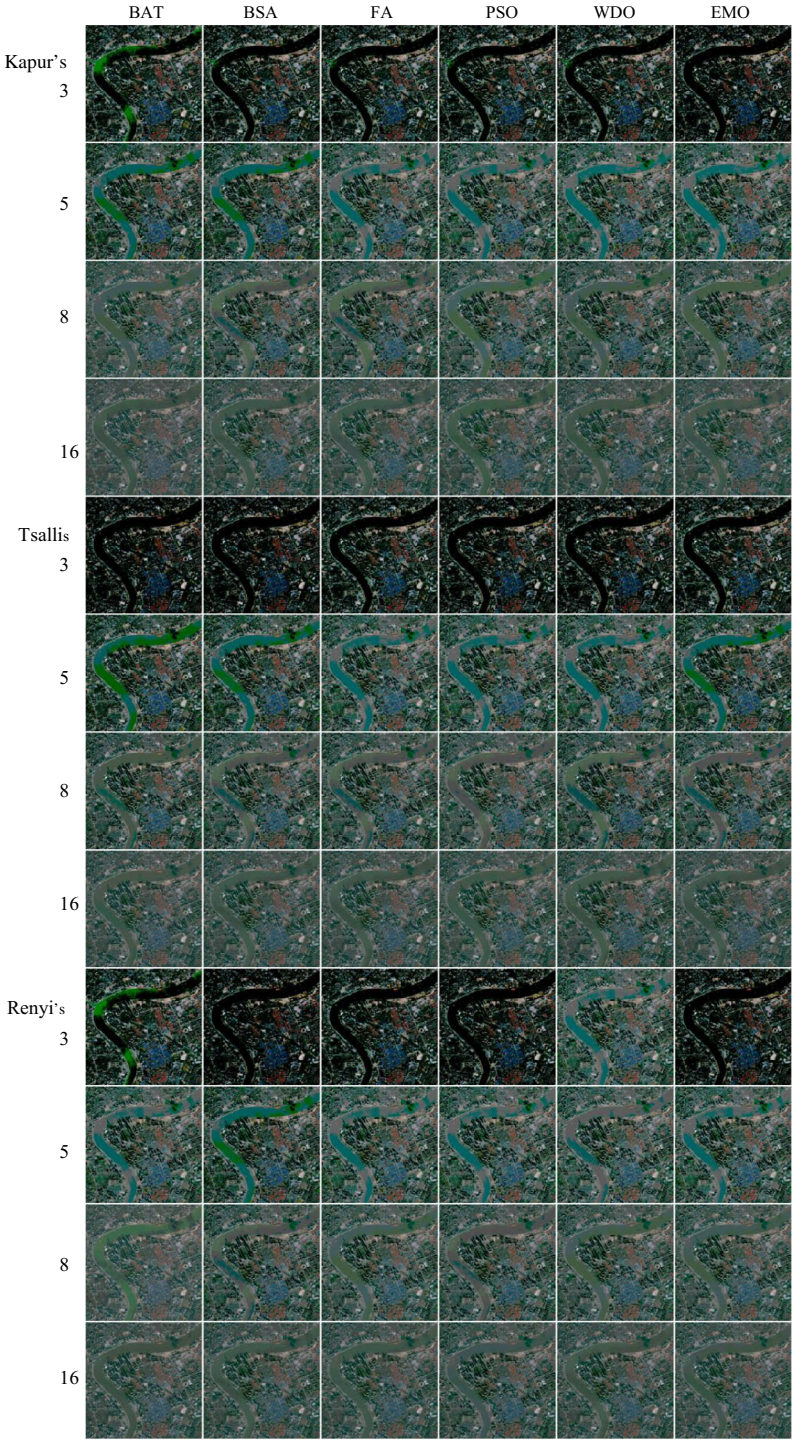

Fig. 11 The 3, 5, 8, 16-levels thresholded test image 7 obtained by BAT, BSA, FA, PSO, WDO, and EMO techniques using Kapur's, Tsallis, and Renyi's entropy

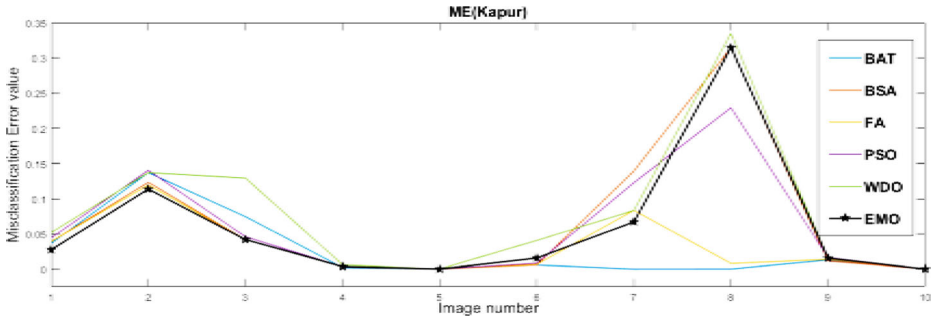

Fig. 12 Comparison of 8-level ME values for Kapur's entropy

4.4 Experiment 1: Kapur's entropy maximization

This part of the paper discusses the outcomes obtained for various satellite and daily-life test images using Kapur's as a fitness function. Table 3 portrays the misclassification error and objective values obtained by BAT algorithm, BSA, FA, PSO, WDO, and EMO. It is examined that the misclassification error evaluated by the EMO method produces the lowest value amongst all the techniques, which are being compared for almost all the images. MSE and PSNR values obtained using the optimization methods have been listed in Table 6 and the comparison is done with the results acquired using BSA, BAT algorithm, FA, PSO, WDO, and

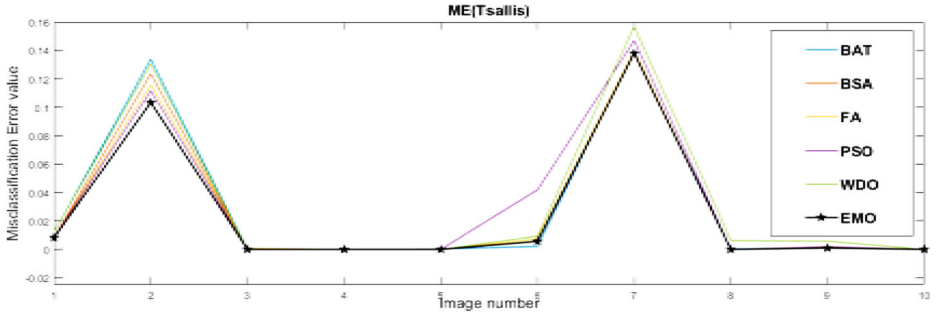

Fig. 13 Comparison of 8-level ME values for Tsallis entropy

EMO methods. Adding to the quality assessment results, the feature assessment parameters

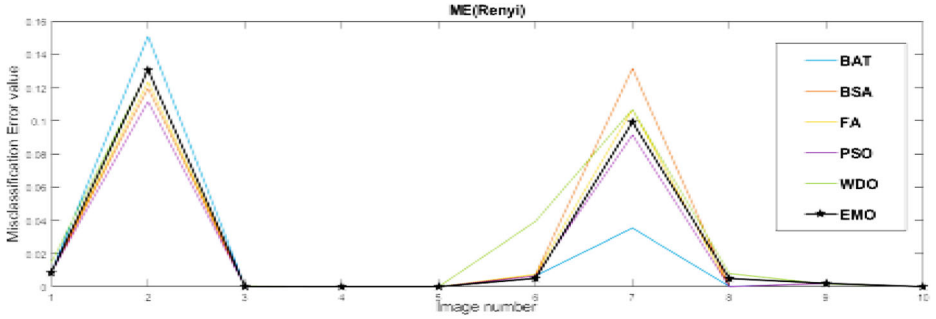

Fig. 14 Comparison of 8-levelME values for Renyi 's entropy

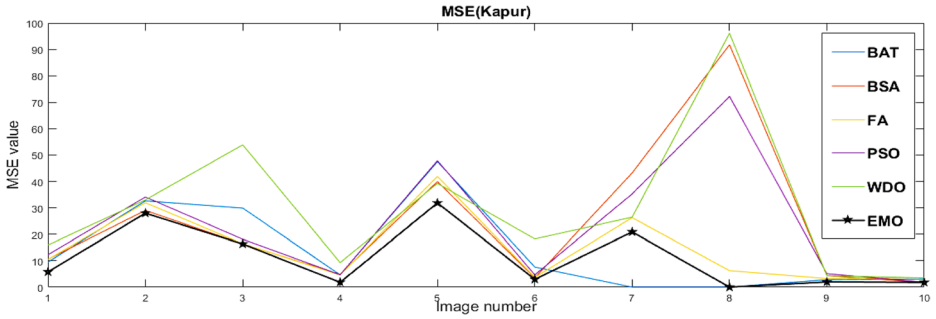

Fig. 15 Comparison of 8-level MSE values for Kapur's entropy

such as SSIM and FSIM also show better results for EMO-Kapur's based segmentation in comparison to other optimization methods, when implemented using Kapur's entropy. This can be seen in Table 9. Table 12 compares the computation efficiency of all the algorithms. This table confirms that the EMO algorithm is the most suitable when it comes to efficiency. Figures 4 and 5 depict the segmented results for all the images obtained at 3-level and 5-level thresholding. Figures 12, 15, 18, 21, 24, shows the plots for the metrics stated above and it can be clearly seen from the plots that the EMO algorithm and Kapur's entropy-based method outperforms all other optimization (BAT algorithm, BSA, FA, WDO, and PSO) techniques with Kapur's entropy for most of the images. The plot for CPU timing is depicted by Fig. 27.

4.5 Experiment 2: Tsallis entropy maximization

In this section, an evaluation of the optimum threshold values from the aid of Tsallis entropy has been discussed for the desired problem. The misclassification error (ME), fitness function values calculated for all the optimization methods used in this paper are listed in Table 4. PSNR and mean square error (MSE) valuation obtained using the BAT algorithm, BSA, FA, PSO, WDO, and EMO with Tsallis entropy is shown in Table 7. A simple observation from Tables 4 and 7 verifies, for most of the images, the best results are obtained when Tsallis entropy is used with electromagnetism-like mechanism optimization. Table 10 compares the similarity in features of the original image and segmented image from the results obtained by using the mentioned methods with Tsallis entropy as an objective function respectively. Figures 6 and 7 portray the segmented results of all considered images for threshold levels3, and 5 acquired for BAT-Tsallis, BSA-Tsallis, FA-Tsallis, PSO-Tsallis, WDO-Tsallis, and

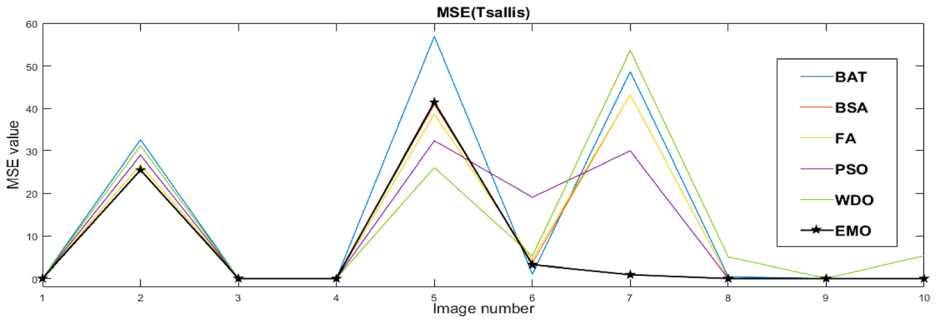

Fig. 16 Comparison of 8-level MSE values for Tsallis entropy

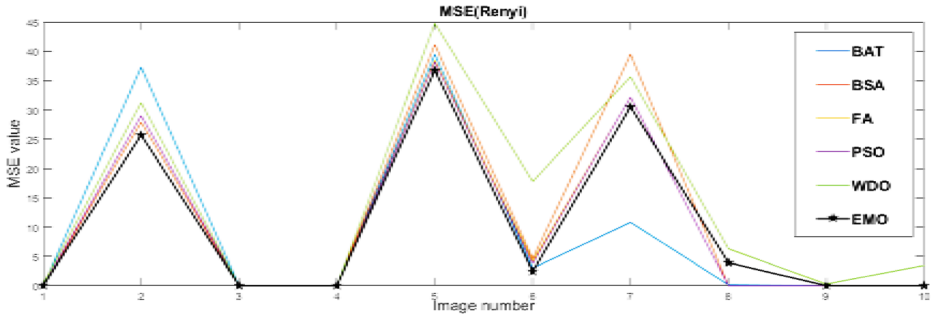

Fig. 17 Comparison of 8-level MSE values for Renyi 's entropy

EMO-Tsallis. Figures 13, 16, 19, 22, 25, and 28 report the plots for the ME, MSE, PSNR, SSIM, FSIM, and CPU timing respectively from which it is clear that the EMO algorithm and Tsallis entropy-based method outperforms all other optimization techniques with Tsallis as a fitness function.

4.6 Experiment 3: Renyi's entropy maximization

In this section of the paper, the results achieved for various test images by using Renyi's entropy as objective (or fitness) function are discussed. Table 5 depicts the objective values and the ME values obtained by BAT algorithm, PSO, WDO, BSA, FA, and EMO algorithm. It has been tested that the misclassification error evaluated by the proposed method i.e. EMO with Renyi entropy harvests the lowest value among all the techniques that are being compared for different standard and satellite images. SSIM and FSIM are the metrics that show the feature similarity between the images being tested. MSE and peak signal to noise ratio PSNR values that have been attained using the proposed Renyi entropy-based EMO method show its supremeness over other methods.

Table 8 contains the comparison of MSE and PSNR of the listed methods whereas Table 11 illustrates the SSIM and FSIM values. Table 12 shows the time required to compute the optimum thresholds by using BSA algorithm, PSO, WDO, FA, BSA, and EMO. From Tables 11 and 12, it has been made sure that EMO-Renyi's beats BAT-Renyi, BSA-Renyi, FA-Renyi, PSO-Renyi, and WDO-Renyi in terms of feature similarity as well as computational efficiency. It can be clearly observed from the segmented images in Figs. 8 (3-level) and 9 (5-level) that the proposed EMO-Renyi's based technique offers superior segmentation when

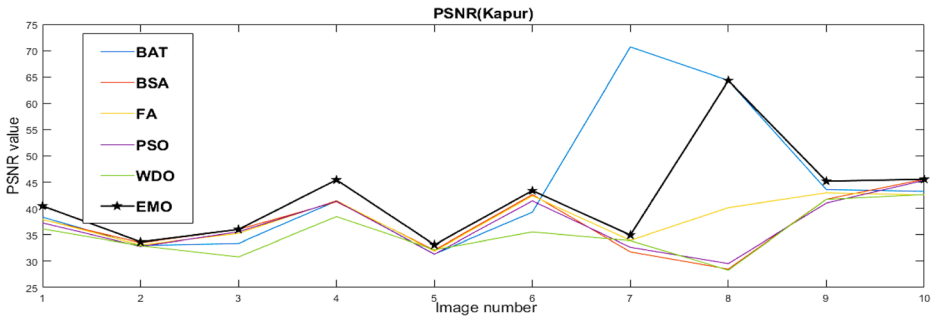

Fig. 18 Comparison of 8-level PSNR values for Kapur's entropy

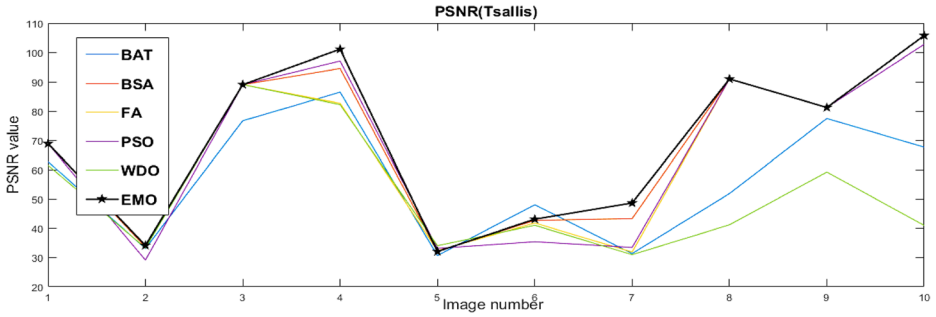

Fig. 19 Comparison of 8-level PSNR values for Tsallis entropy

compared with other evolutionary algorithms such as BSA, BAT algorithm, PSO, FA, and WDO. From the plots presented in Figs. 14, 17, 20, 23, 26, and 29 depict the qualitative and computational supremacy of the proposed method over other methods.

4.7 Comparative analysis of Renyi's, Tsallis, and Kapur's entropy

Keeping the view of all the fidelity assessment from Tables 3, 4, 5, 6, 7, 8, 9, 10, and 11, EMO-Kapur's, EMO-Tsallis, and EMO-Renyi's have performed outstandingly in comparison to BAT algorithm, BSA, FA, PSO, and WDO. In addition, Fig. 10 shows the segmented results of the second test image at 3-level, 5-level, 8-level, and 16-level thresholding from which it can be deduced that EMO-Renyi's method surpasses the EMO-Kapur's and EMO-Tsallis. The same can be concluded from Fig. 11 which shows segmented results for test image 7 which is a satellite image, it has been clarified that Renyi's entropy-based segmentation performs in a better manner in comparison with Kapur's and Tsallis entropy-based multilevel thresholding approaches. Table 12 has been computed to show the computational efficiency among all algorithms when implemented with the aid of Renyi's, Tsallis, and Kapur's entropy as fitness (or objective) function. From Table 12, it can be clearly visualized that Renyi's entropy outsmarts Kapur's and Tsallis and also that the proposed method i.e. EMO-Renyi's is the absolute suitable when the time is the most important matter of concern. The same has also been depicted in the plot in Fig. 30 for 8-level and Fig. 31 for 16-level which implies the computational supremacy of EMO-Renyi's based color image segmentation. The convergence plots at 8-level for input images 3, 4, 8, and 10 have been shown in Fig. 32a–d. From the convergence graph plots for each objective function, it can be easily observed that for mostly

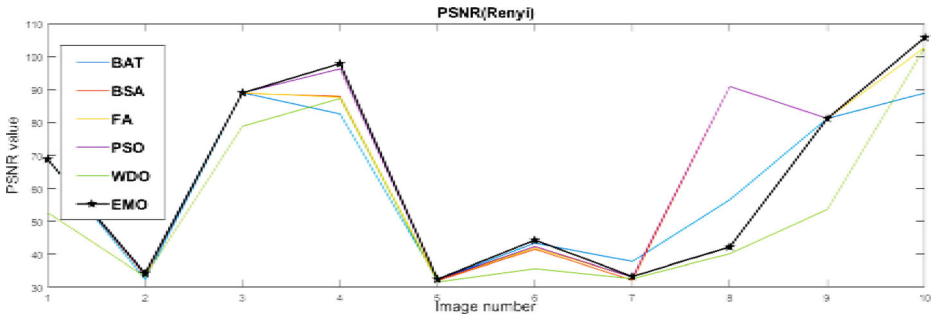

Fig. 20 Comparison of 8-level PSNR values for Renyi 's entropy

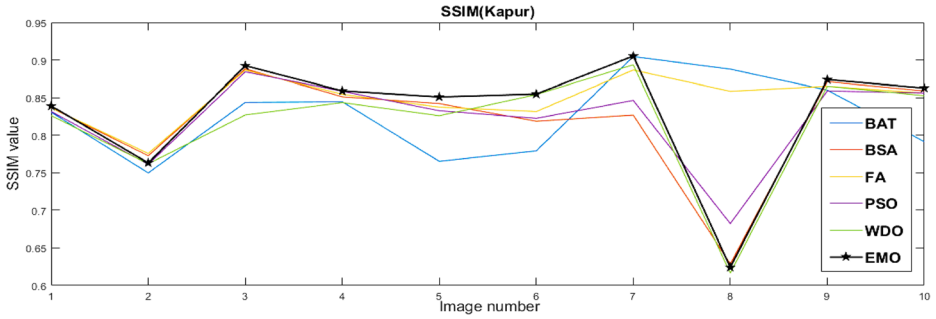

Fig. 21 Comparison of 8-level SSIM values for Kapur's entropy

all the images EMO-Renyi's technique is converging faster than rest of the algorithms used in this paper.

In order to measure the performance of the proposed approach, mean square error (MSE), misclassification error (ME), SSIM, FSIM, and PSNR have been utilized to assess the quality of segmentation, considering the coincidences in between the original images and respective segmented images. After the analysis of the convergence rate of different images using EMO, FA, PSO, BAT algorithm, BSA, and WDO algorithms, it is concluded that EMO is very fast as compared to other algorithms. The order of computational efficiency has been sorted in the order as EMO > FA > WDO > PSO > BAT algorithm > BSA. Even if individual entropies are considered, EMO outperforms all other optimization techniques considered in this paper. Hence, EMO has been proven to be superior to the rest of algorithms and also the EMO-Renyi's beats EMO-Tsallis and EMO-Kapur's i.e. in terms of efficiency and robustness Renyi's > Kapur's > Tsallis.

In addition, convergence plots have been drawn in Fig. 32 for Kapur's, Tsallis and Renyi's entropy. As seen from all of the convergence plots, the optimum value (maximum value) is attained in the case of proposed EMO-Renyi's method. Proposed EMO-Renyi computes maximum value efficiently in comparison with the BAT, BSA, FA, PSO, and WDO algorithms.

4.8 Merits of the proposed method

The color image multilevel thresholding outcomes of proposed EMO-Renyi's method are encouraging and it inspires future works. For statistical independent subsystems, Renyi's

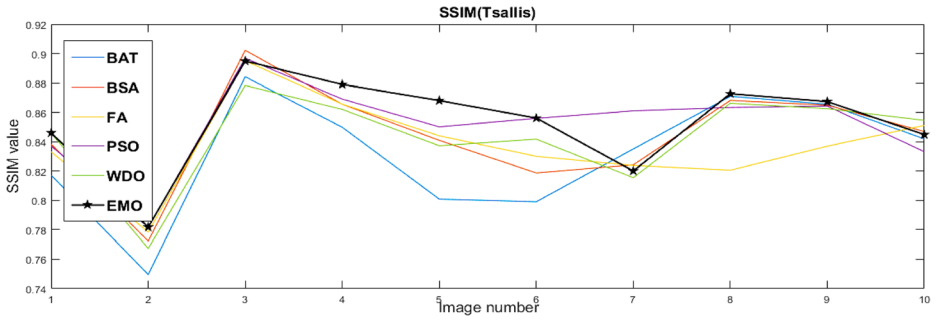

Fig. 22 Comparison of 8-level SSIM values for Tsallis entropy

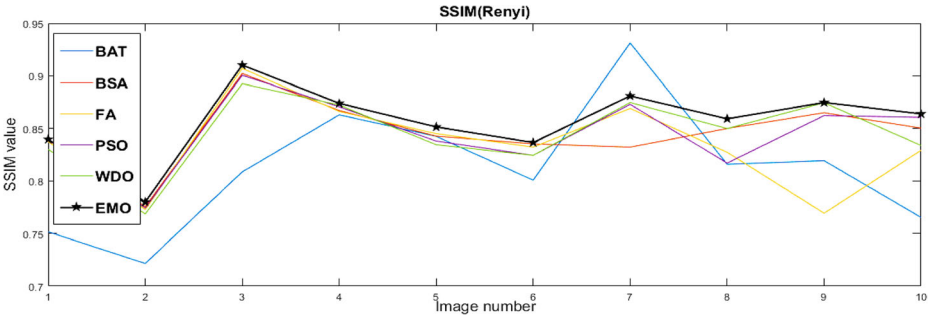

Fig. 23 Comparison of 8-level SSIM values for Renyi 's entropy

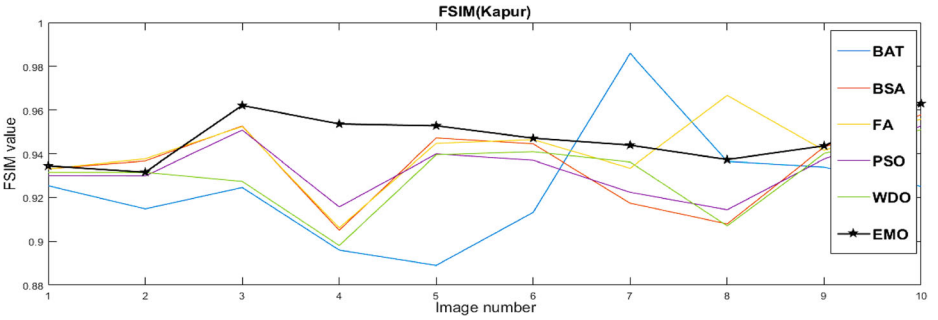

Fig. 24 Comparison of 8-level FSIM values for Kapur's entropy

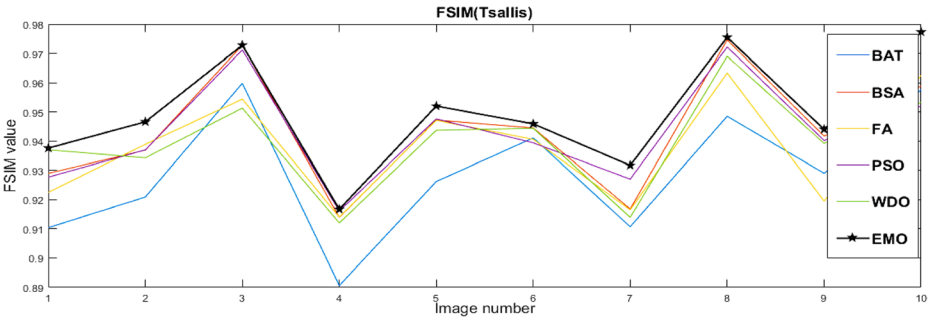

Fig. 25 Comparison of 8-level FSIM values for Tsallis entropy.

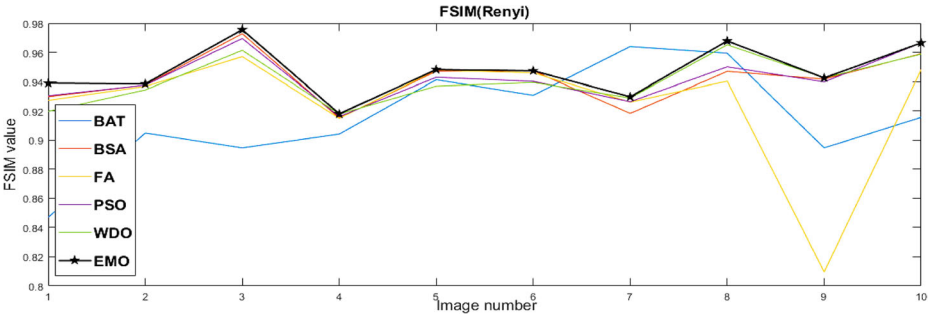

Fig. 26 Comparison of 8-level FSIM values for Renyi 's entropy

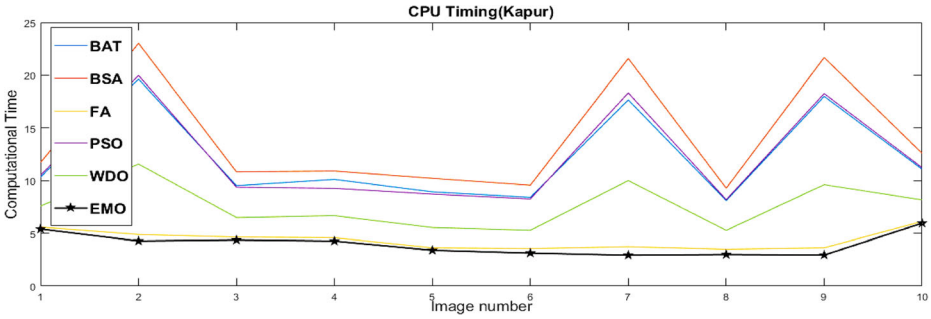

Fig. 27 Comparison of 8-level CPU time for Kapur's entropy

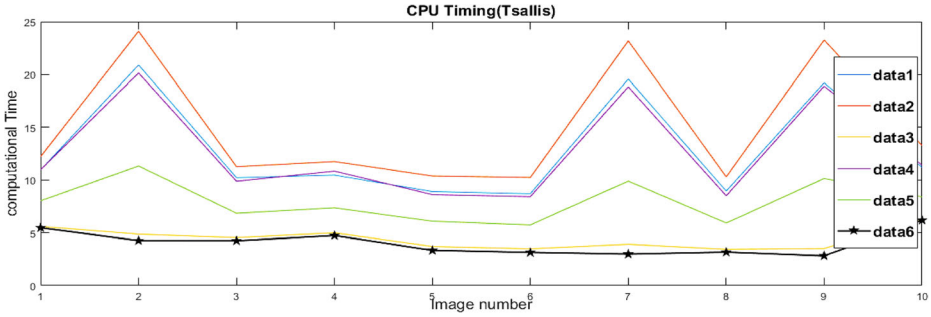

Fig. 28 Comparison of 8-level CPU time for Tsallis entropy

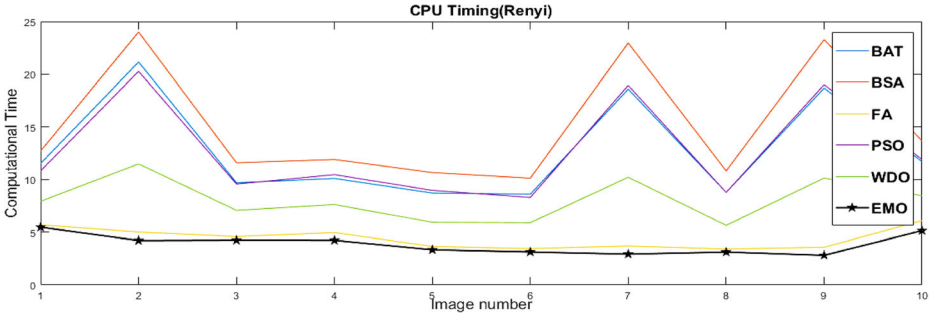

Fig. 29 Comparison of 8-level CPU time for Renyi 's entropy

entropy shows an extensive property and is applied to find the best threshold value for image segmentation. However, EMO belongs to old optimization technique but by combining this technique with Renyi's entropy this produces efficient segmentation results with high accuracy. This technique has a fast convergence rate. Renyi's entropy has selected for energy calculations because of the easiest implementation and the highest accuracy. The easy extension of Renyi's entropy to multilevel thresholding problems sums up the advantage of less computation cost. The proposed work has noteworthy application in the area of expert and intelligent systems which includes machine learning, medical image processing, object

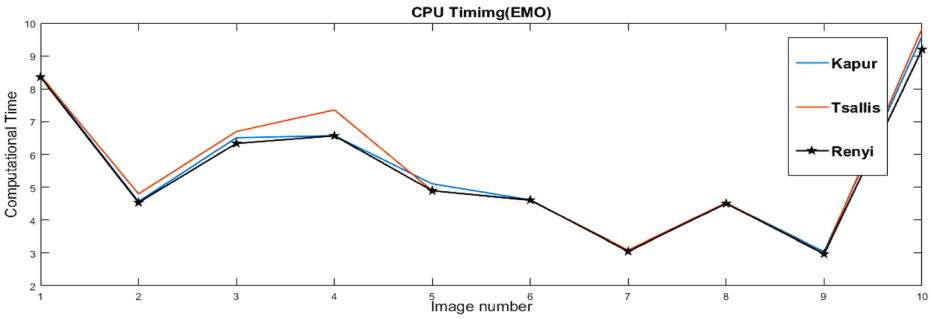

Fig. 30 Comparison of CPU time required by EMO algorithm using Kapur's, Tsallis and Renyi's entropy at 8-level threshold

recognition, traffic monitoring practice, video investigation, the study of thermal imaging, pattern analysis, image and computer vision domain. So far, multilevel-based image segmentation approaches have been effectively utilized in several fields of expert and intelligent systems applications with a different purpose. Few of them may consider as face recognition, image retrieval, and object detection for example. Satellite images are often segmented in the presence of unpredictability. This randomness is due to the factors that are highly dependent on environmental conditions, deprived resolution, very low spatial resolution, and poor illumination.

5 Conclusion

This paper has focused on color image multilevel thresholding for normal data and satellite test images using current optimization algorithms. In this paper, EMO, BAT algorithm, BSA, FA, PSO, and WDO methods have been employed to maximize Renyi's, Tsallis, and Kapur's entropy to solve the problem of multilevel thresholding by determining the optimum multilevel threshold values. Based on qualitative and quantitative assessments, it can expose that the proposed EMO-Renyi's algorithm can be efficiently and effectively useful in multilevel thresholding for satellite and daily-life color images. The outcomes emphasize that the EMO

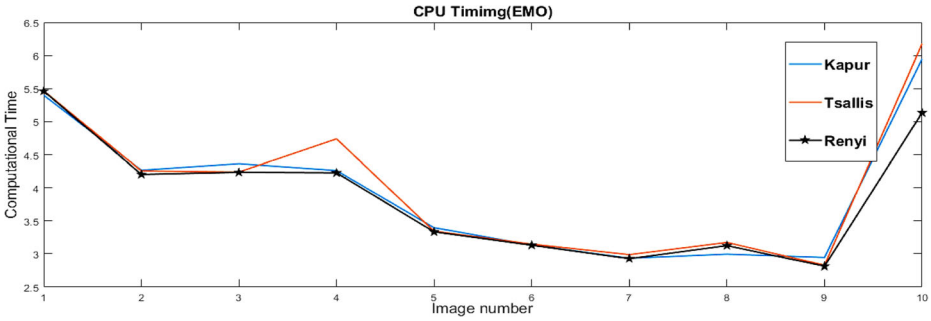

Fig. 31 Comparison of CPU time required by EMO algorithm using Kapur's, Tsallis and Renyi's entropy at 16-level threshold

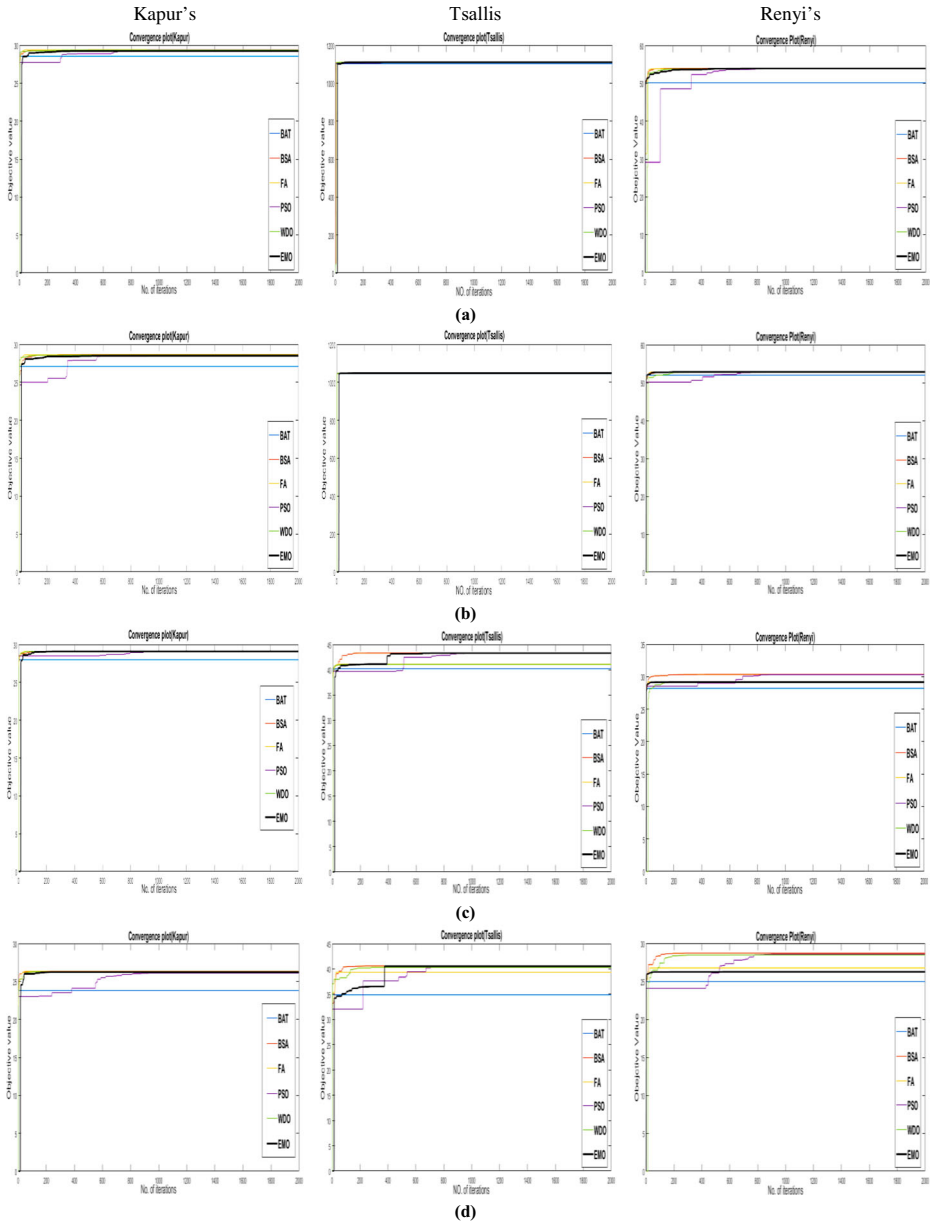

Fig. 32 **a-d** Convergence plot for BAT, BSA, FA, PSO, WDO and EMO at 8-level threshold for input image 3, 4, 8, and 10 respectively

outperforms the BAT algorithm, BSA, FA, PSO, and WDO when implemented with each of the objective function. The best part of EMO is its computational proficiency for multilevel color image segmentation over existing approaches. The experimental outcomes are encouraging and motivate futuristic research areas to apply the EMO algorithm to other image processing applications such as image enhancement and image denoising for remote sensing images, image classification and in various computer-related problems. Furthermore, the

proposed scheme can be extended for medical image segmentation due to fast segmentation ability.

Acknowledgments The authors wish to thank all reviewers, editor and associate editor for their fruitful comments and suggestions for significant improvement of the manuscript.

References

1. Agrawal S, Panda R, Bhuyan S, Panigrahi BK (2013) Tsallis entropy based optimal multilevel thresholding using cuckoo search algorithm. Swarm Evol Comput 11:16–30
2. Aja-Fernández S, Curiale AH, Vegas-Sánchez-Ferrero G (2015) A local fuzzy thresholding methodology for multiregion image segmentation. Knowl-Based Syst 83:1–12
3. Bhandari AK (2018) A novel beta differential evolution algorithm-based fast multilevel thresholding for color image segmentation. Neural Comput & Applic 1–31
4. Bhandari AK, Kumar IV (2019) A context sensitive energy thresholding based 3D Otsu function for image segmentation using human learning optimization. Appl Soft Comput 1–35
5. Bhandari AK, Rahul K (2019) A context sensitive Masi entropy for multilevel image segmentation using moth swarm algorithm. Infrared Phys Technol 98:132–154
6. Bhandari AK, Rahul K (2019) A novel local contrast fusion-based fuzzy model for color image multilevel thresholding using grasshopper optimization. Appl Soft Comput 81:1–31
7. Bhandari AK, Soni V, Kumar A, Singh GK (2014) Artificial bee colony-based satellite image contrast and brightness enhancement technique using DWT-SVD. Int J Remote Sens 35(5):1601–1624
8. Bhandari AK, Singh VK, Kumar A, Singh GK (2014) Cuckoo search algorithm and wind driven optimization based study of satellite image segmentation for multilevel thresholding using Kapur's entropy. Expert Syst Appl 41(7):3538–3560
9. Bhandari AK, Kumar A, Singh GK (2015a) Modified artificial bee colony based computationally efficient multilevel thresholding for satellite image segmentation using Kapur's, Otsu and Tsallis functions. Expert Syst Appl 42(3):1573–1601
10. Bhandari AK, Kumar A, Singh GK (2015b) Tsallis entropy based multilevel thresholding for colored satellite image segmentation using evolutionary algorithms. Expert Syst Appl 42(22):8707–8730
11. Bhandari AK, Kumar A, Chaudhary S, Singh GK (2016) A novel color image multilevel thresholding based segmentation using nature inspired optimization algorithms. Expert Syst Appl 63:112–133
12. Bhandari AK, Kumar A, Singh GK, Soni V (2016) Performance study of evolutionary algorithm for different wavelet filters for satellite image denoising using sub-band adaptive threshold. J Exp Theor Artif Intell 28(1–2):71–95
13. Bhandari AK, Kumar A, Chaudhary S, Singh GK (2017) A new beta differential evolution algorithm for edge preserved colored satellite image enhancement. Multidim Syst Sign Process 28(2):495–527
14. Bhandari AK, Maurya S, Meena AK (2018) Social spider optimization based optimally weighted Otsu thresholding for image enhancement. IEEE J Sel Topics Appl Earth Observ Remote Sens 1–13
15. Bhandari AK, Kumar IV, Srinivas K (2019) Cuttlefish algorithm based multilevel 3D Otsu function for color image segmentation. IEEE Trans Instrum Meas 1–10
16. Bhandari AK, Singh A, Kumar IV (2019) Spatial context energy curve-based multilevel 3-D Otsu algorithm for image segmentation. IEEE Trans Syst, Man, Cybern, Syst 1–14
17. Birbil Şİ, Fang SC (2003) An electromagnetism-like mechanism for global optimization. J Glob Optim 25(3):263–282
18. Birbil SI, Fang SC, Sheu RL (2004) On the convergence of a population-based global optimization algorithm. J Glob Optim 30:301–318
19. Bouaziz A, Draa A, Chikhi S (2015) Artificial bees for multilevel thresholding of iris images. Swarm Evol Comput 21:32–40
20. Chao Y, Dai M, Chen K, Chen P, Zhang Z (2016) A novel gravitational search algorithm for multilevel image segmentation and its application on semiconductor packages vision inspection. Optik Int J Light Electron Opt 127(14):5770–5782
21. Choy SK, Lam SY, Yu KW, Lee WY, Leung KT (2017) Fuzzy model-based clustering and its application in image segmentation. Pattern Recogn 68:141–157

22. Civicioglu P (2013) Backtracking search optimization algorithm for numerical optimization problems. Appl Math Comput 219(15):8121–8144
23. De Albuquerque MP, Esquef IA, Mello AG (2004) Image thresholding using Tsallis entropy. Pattern Recogn Lett 25(9):1059–1065
24. De Castro LN, Von Zuben FJ (2002) Learning and optimization using the clonal selection principle. IEEE Trans Evol Comput 6(3):239–251
25. Dey S, Bhattacharyya S, Maulik U (2016) New quantum inspired meta-heuristic techniques for multi-level colour image thresholding. Appl Soft Comput 46:677–702
26. Dey S, Bhattacharyya S, Maulik U (2017) Efficient quantum inspired meta-heuristics for multi-level true colour image thresholding. Appl Soft Comput 56(C):472–513
27. Fan F, Ma Y, Li C, Mei X, Huang J, Ma J (2017) Hyperspectral image denoising with superpixel segmentation and low-rank representation. Inf Sci 397:48–68
28. Gandomi AH, Yang XS, Alavi AH (2011) Mixed variable structural optimization using firefly algorithm. Comput Struct 89(23–24):2325–2336
29. He L, Huang S (2017) Modified firefly algorithm based multilevel thresholding for color image segmentation. Neurocomputing 240:152–174
30. Huo F, Liu Y, Wang D, Sun B (2017) Bloch quantum artificial bee colony algorithm and its application in image threshold segmentation. SIViP 11(8):1585–1592
31. Ishak AB (2017) Choosing parameters for Rényi and Tsallis entropies within a two-dimensional multilevel image segmentation framework. Physica A 466:521–536
32. Kandhway P, Bhandari AK (2019) Spatial context cross entropy function based multilevel image segmentation using multi-verse optimizer. Multimed Tools Appl 1–29
33. Kapur JN, Sahoo PK, Wong AK (1985) A new method for gray-level picture thresholding using the entropy of the histogram. CVGIP 29(3):273–285
34. Lahmiri S (2017) Glioma detection based on multi-fractal features of segmented brain MRI by particle swarm optimization techniques. Biomed Signal Process Control 31:148–155
35. Li Y, Bai X, Jiao L, Xue Y (2017) Partitioned-cooperative quantum-behaved particle swarm optimization based on multilevel thresholding applied to medical image segmentation. Appl Soft Comput 56:345–356
36. Mishra S, Panda M (2018) Bat algorithm for multilevel colour image segmentation using entropy-based thresholding. Arab J Sci Eng 1–30
37. Nie F, Zhang P, Li J, Ding D (2017) A novel generalized entropy and its application in image thresholding. Signal Process 134:23–34
38. Oliva D, Cuevas E, Pajares G, Zaldivar D, Osuna V (2014) A multilevel thresholding algorithm using electromagnetism optimization. Neurocomputing 139:357–381
39. Oliva D, Osuna-Enciso V, Cuevas E, Pajares G, Pérez-Cisneros M, Zaldívar D (2015) Improving segmentation velocity using an evolutionary method. Expert Syst Appl 42(14):5874–5886
40. Otsu N (1979) A threshold selection method from gray-level histograms. IEEE Trans Syst, Man, Cybern 9(1):62–66
41. Ouadfel S, Taleb-Ahmed A (2016) Social spiders optimization and flower pollination algorithm for multilevel image thresholding: a performance study. Expert Syst Appl 55:566–584
42. Pare S, Bhandari AK, Kumar A, Singh GK, Khare S (2015) Satellite image segmentation based on different objective functions using genetic algorithm: a comparative study. In: 2015 IEEE international conference on digital signal processing (DSP). IEEE, p 730–734
43. Pare S, Kumar A, Bajaj V, Singh GK (2016) A multilevel color image segmentation technique based on cuckoo search algorithm and energy curve. Appl Soft Comput 47:76–102
44. Pare S, Bhandari AK, Kumar A, Bajaj V (2017) Backtracking search algorithm for color image multilevel thresholding. SIViP 1–8
45. Pare S, Bhandari AK, Kumar A, Singh GK (2017a) A new technique for multilevel color image thresholding based on modified fuzzy entropy and Lévy flight firefly algorithm. Comput Electr Eng 70, 476-495
46. Pare S, Bhandari AK, Kumar A, Singh GK (2017b) An optimal color image multilevel thresholding technique using Grey-level co-occurrence matrix. Expert Syst Appl 87:335–362
47. Rajathilagam B, Rangarajan M (2017) Edge detection using G-lets based on matrix factorization by group representations. Pattern Recogn 67:1–15
48. Rajinikanth V, Satapathy SC (2018) Segmentation of ischemic stroke lesion in brain MRI based on social group optimization and fuzzy-Tsallis entropy. Arab J Sci Eng 1–14
49. Rajinikanth V, Raja NSM, Satapathy SC (2016) Robust color image multi-thresholding using between-class variance and cuckoo search algorithm. In: Information systems design and intelligent applications. Springer, New Delhi, pp 379–386

50. Sahoo PK, Arora G (2004) A thresholding method based on two-dimensional Renyi's entropy. Pattern Recogn 37(6):1149–1161
51. Sahoo PK, Soltani SAKC, Wong AK (1988) A survey of thresholding techniques. CVGIP 41(2):233–260
52. Sahoo P, Wilkins C, Yeager J (1997) Threshold selection using Renyi's entropy. Pattern Recogn 30(1):71–84
53. Sarkar S, Das S, Chaudhuri SS (2016) Hyper-spectral image segmentation using Rényi entropy based multi-level thresholding aided with differential evolution. Expert Syst Appl 50:120–129
54. Suresh S, Lal S (2016) An efficient cuckoo search algorithm based multilevel thresholding for segmentation of satellite images using different objective functions. Expert Syst Appl 58:184–209
55. Suresh S, Lal S (2017) Multilevel thresholding based on chaotic Darwinian particle swarm optimization for segmentation of satellite images. Appl Soft Comput 55:503–522
56. Tsai WH (1985) Moment-preserving thresolding: a new approach. CVGIP 29(3):377–393
57. Yuan B, Zhang C, Shao X, Jiang Z (2015) An effective hybrid honey bee mating optimization algorithm for balancing mixed-model two-sided assembly lines. Comput Oper Res 53:32–41
58. Zhang J, Ehinger KA, Wei H, Zhang K, Yang J (2017) A novel graph-based optimization framework for salient object detection. Pattern Recogn 64:39–50

Ashish Kumar Bhandari received the B. Tech degree in electronics and communication engineering from Mahatma Jyotiba Phule Rohilkhand University, Bareilly, India, in 2009 and M. Tech and Ph.D. (Gold Medalist) degrees from Indian Institute of Information Technology Jabalpur, India in 2011 and 2015, respectively. Currently, he is assistant professor in the electronics and communication engineering department, National Institute of Technology Patna, Bihar, (India). His research interests include image enhancement and image segmentation. Dr. Bhandari is the Reviewer of the IEEE transactions and journals, including the IEEE Transactions on Cybernetics, the IEEE Transactions on NanoBioscience, the IEEE Transactions on Systems, Man and Cybernetics: Systems, the IEEE Transactions on Multimedia, the IEEE Journal of Selected Topics in Applied Earth Observations and Remote Sensing, Swarm and Evolutionary Computation, Applied Soft Computing, Signal Processing, Digital Signal Processing, IET Image Processing, Soft Computing, and Signal, Image and Video Processing.

Neha Singh received the B. Tech degree in electronics and communication engineering from Magadh University, Bodh-Gaya, Bihar, (India) in 2011 and M. Tech degree from Motilal Nehru National Institute of Technology Allahabad, U.P (India) in 2015. Currently, she is pursuing Ph.D. in Electronics and Communication Engineering, from National Institute of Technology Patna, Bihar, (India). Her research interests include image enhancement and image segmentation.

Swapnil Shubham has received the B. Tech in Electronics & Communication Engineering from Kalinga Institute of Industrial Technology, KIIT University, Bhubaneswar, Odisha, India, His research interests include image segmentation using multilevel thresholding and optimization techniques.

Affiliations

Ashish Kumar Bhandari[1] · **Neha Singh**[1] · **Swapnil Shubham**[1]

Neha Singh
nehasingh0910@gmail.com

Swapnil Shubham
swapnil612chi@gmail.com

[1] Department of Electronics and Communication Engineering, National Institute of Technology Patna, Patna 800005, India